

**A PROBABILISTIC APPROACH TO ASSESS HYDRATE FORMATION AND  
DESIGN PREVENTIVE MEASURES**

by

© Dinesh Bandara Herath

A Thesis submitted to the

School of Graduate Studies

in partial fulfilment of the requirements for the degree of

**Master of Engineering**

**Faculty of Engineering and Applied Science**

**Memorial University of Newfoundland**

**May 2016**

St. John's

Newfoundland

## **Abstract**

Formation of hydrates is one of the major flow assurance problems faced by the oil and gas industry. Hydrates tend to form in natural gas pipelines with the presence of water and favorable temperature and pressure conditions, generally low temperatures and corresponding high pressures. Agglomeration of hydrates can result in blockage of flowlines and equipment, which can be time consuming to remove in subsea equipment and cause safety issues. Natural gas pipelines are more susceptible to burst and explosion owing to hydrate plugging. Therefore, a rigorous risk-assessment related to hydrate formation is required, which assists in preventing hydrate blockage and ensuring equipment integrity. This thesis presents a novel methodology to assess the probability of hydrate formation and presents a risk-based approach to determine the parameters of winterization schemes to avoid hydrate formation in natural gas pipelines operating in Arctic conditions. It also presents a lab-scale multiphase flow loop to study the effects of geometric and hydrodynamic parameters on hydrate formation and discusses the effects of geometric and hydrodynamic parameters on multiphase development length of a pipeline. Therefore, this study substantially contributes to the assessment of probability of hydrate formation and the decision making process of winterization strategies to prevent hydrate formation in Arctic conditions.

## **Acknowledgement**

First and foremost I am very grateful to my supervisor Dr. Faisal Khan, for the continuous support, guidance and encouragement he gave me and also for the financial support provided. I acknowledge with gratitude the valuable suggestions and feedback in preparation of the manuscripts given by Dr. Aziz Rahman and Dr. Ming Yang. Also, I greatly acknowledge the funding received by Vale research grant, Research and Development Corporation (RDC) of Newfoundland and Labrador, Natural Science and Engineering Research Council (NSERC) of Canada and School of Graduate Studies, Memorial University.

Furthermore, I highly appreciate the support given by the research and administration staff of the Faculty of Engineering and Applied Science, Memorial University. Especially Dr. Leonard Lye, Moya Crocker, Coleen Mahoney and everyone who helped me in some way. My heartfelt thanks also goes to all my friends and colleagues for their continuous support from the beginning, Samith Rathnayaka, Dan Chen, Oscar De Silva, Pradeep Dalpatadu and Migara Liyanage.

Finally, I would like to thank my loving and supportive wife, Kasuni Liyanage, my parents and my sister for all the love and support. Thank you!

## Table of Contents

Abstract.....	ii
Acknowledgement .....	iii
Table of Contents.....	iv
List of Tables .....	viii
List of Figures.....	ix
List of Appendices .....	xi
List of Symbols, Nomenclature or Abbreviations .....	xii
Introduction and Overview .....	1
Co-authorship Statement.....	4
Chapter 1. Hydrate Formation.....	5
1.1 Hydrates .....	5
1.2 Hydrate forming conditions .....	6
1.3 Types of Hydrates .....	8
1.4 Indications of hydrate formations in pipelines under different operating conditions .....	10
1.5 Hydrate formation in Subsea Safety Equipment.....	11
1.6 Hydrate prevention.....	13

1.7	Predicting hydrate forming conditions .....	15
1.8	K-factor method .....	16
1.8.1	Gas gravity method.....	16
1.8.2	Correlations based on gas gravity method.....	16
1.9	References .....	19
Chapter 2. Probabilistic Estimation of Hydrate Formation .....		22
2.1	Introduction .....	23
2.2	Hydrate formation probability estimation method.....	27
2.2.1	Calculation of hydrate forming conditions .....	27
2.2.2	Shortest Path of Hydrate Formation (SPHF) .....	29
2.2.3	Definition of safe temperature and pressure .....	30
2.3	Hydrate formation probability calculations.....	33
2.3.1	Case Study I.....	35
2.3.2	Case study II .....	38
2.4	Validation of the proposed method .....	40
2.5	Conclusions .....	43
2.6	References .....	45
Chapter 3. Risk-based Winterization to Prevent Hydrate Formation in Northern Harsh Environment 48		

3.1	Introduction .....	49
3.2	Hydrate Formation .....	52
3.3	Risk-based Winterization Approach to Prevent Hydrate Formation .....	54
3.3.1	Identify the criticality of the system .....	54
3.3.2	Environmental load.....	55
3.3.3	Estimation of Probability of Hydrate Formation (PoHF) .....	57
3.3.4	Risk estimation.....	61
3.3.5	Winterization methods .....	62
3.3.6	Estimation of Efficacy of Winterization .....	66
3.4	Determine the parameters of winterization schemes.....	67
3.4.1	Physics behind heat loss from natural gas pipelines.....	68
3.4.2	Determination of inhibitor percentage requirement.....	71
3.4.3	Determination of heat trace capacity and insulation thickness.....	72
3.5	Discussion .....	76
3.6	Conclusions .....	78
3.7	References .....	80
Chapter 4.	Multiphase Hydrate Induction Experiment in a Subsea Pipeline .....	83
4.1	Introduction .....	84
4.2	Lab-Scale Flow Loop.....	87

4.3	Development Length .....	89
4.3.1	Homogeneous Reynolds number .....	90
4.3.2	Three-phase Reynolds number .....	92
4.3.3	Slurry flow .....	93
4.4	Results and Discussions .....	94
4.5	Conclusions .....	99
4.6	References .....	100
Chapter 5.	Summary .....	103
Appendix	.....	106

## **List of Tables**

Table 2-1: Percentage deviation of average difference from the mean .....	42
Table 3-1: Parameters used in case study .....	73

## List of Figures

Figure 1-1: Hydrate forming conditions .....	7
Figure 1-2: Hydrate forming curves for different inhibition levels .....	8
Figure 1-3: Hydrate structures .....	9
Figure 1-4: Different operating conditions where hydrates tend to form .....	10
Figure 1-5: Permissible expansion of a 0.6 gravity natural gas without hydrate formation (Katz, 1945) .....	12
Figure 1-6: Pressure-Temperature curves for predicting hydrate formation (Katz, 1945)	18
Figure 2-1: Methodology for the estimation of probability of hydrate formation .....	28
Figure 2-2: Possible shortest pathways.....	29
Figure 2-3: Algorithm to obtain achievable pathways using SPHF .....	32
Figure 2-4: Calculation method .....	34
Figure 2-5: (a) Probability values for 99% CH <sub>4</sub> & 1% C <sub>2</sub> H <sub>6</sub> , (b) Probability values for 99% CH <sub>4</sub> , 1% C <sub>2</sub> H <sub>6</sub> & MeOH 10 wt% .....	37
Figure 2-6: Hydrate formation probability curves .....	37
Figure 2-7: Deepwater pipeline with hydrate curves (Notz, 1994) .....	38
Figure 2-8: (a) Probability values without inhibition, (b) Probability values with MeOH 20 wt% .....	39
Figure 2-9: Average difference between probability curves.....	41
Figure 3-1: Factors affecting the decision making process of winterization .....	50
Figure 3-2: Deepwater pipeline with hydrate curves [Notz, 1994] .....	53
Figure 3-3: Risk-based winterization approach to prevent hydrate formation .....	56

Figure 3-4: Risk matrix.....	57
Figure 3-5: Method to obtain the minimum allowable temperature difference.....	59
Figure 3-6: Hydrate formation curve- Minimum allowable temperature .....	60
Figure 3-7: Pipe configuration .....	68
Figure 3-8: Insulation Thickness Vs Heat Trace Wattage .....	75
Figure 4-1: Basic process flow chart of multiphase flow loop and hydrate induction experiment.....	86
Figure 4-2: Process flow diagram of proposed flow loop PR-Pressure Regulator; F-Flow Meter, P-Pressure Transmitter; T-Temperature Transmitter; S-Solid Particles; V-View Port.....	88
Figure 4-3: Slurry superficial velocity Vs ratio of entrance length to pipe diameter with varying void fractions .....	95
Figure 4-4: Slurry superficial velocity Vs ratio of entrance length to pipe diameter with varying solid concentrations .....	96
Figure 4-5: Slurry superficial velocity ratio Vs Entrance length to pipe diameter with varying pipe diameters .....	96
Figure 4-6: Slurry superficial velocity Vs ratio of entrance length to pipe diameter with varying liquid viscosity.....	97
Figure 4-7: Slurry superficial velocity Vs ratio of entrance length to pipe diameter with varying liquid density .....	98

## **List of Appendices**

Appendix A: Parameters of combined winterization approach.....	106
Appendix B: Derivation of equations.....	107

## List of Symbols, Nomenclature or Abbreviations

ABS	American Bureau of Shipping
DNV	Norwegian Classification Society
ISO	International Organization for Standardization
HET	Hydrate Equilibrium temperature
PoHF	Probability of Hydrate Formation
RMRS	Russian Classification Society
SSV	Subsea Safety Valve
SPHF	Shortest Path of Hydrate Formation
<i>A</i>	Area
<i>C</i>	Solid concentration (%)
CH <sub>4</sub>	Methane
C <sub>2</sub> H <sub>6</sub>	Ethane
<i>D</i>	Pipe diameter
F	Fahrenheit

H	Heat transfer coefficient
M	Molar mass of inhibitor
$\dot{M}_{(y)}$	Local mass flow rate
MeOH	Methanol
Nu	Nusselt number
Pr	Prandtl number
$P_{SP}$	Pressure at safe point
$P_i$	Pressure at intersecting point
$P_{OP}$	Pressure at operating point
$P_{md}$	Mean difference between safe pressure and average pressure on hydrate equilibrium curve
$Re_D$	Reynolds number
S	Slip ratio
$T_{eq}$	Hydrate equilibrium temperature
$\Delta T_{system}$	The difference between the load and the operating envelop
$\Delta T_{min}$	The minimum allowable temperature difference between the load and the operating temperature to maintain the system in the hydrate free region

$T_i$	Temperature at intersecting point
$T_{md}$	Mean difference between safe temperature and average temperature on hydrate equilibrium curve
$T_{OP}$	Temperature at operating point
$T_{SP}$	Temperature at safe point
U	Overall heat transfer coefficient
$u_{(y)}$	Local velocity
$u_{(y)}^S$	Local superficial velocity
$u_{3-p}$	Three-phase mixture velocity
W	Concentration of the inhibitor in weight percent in the aqueous phase
$W_e$	Winterization efficacy
$x$	Mass quality
$x_{MeOH}$	Mole fraction of inhibitor in liquid phase, wt%
$\mu$	Mean
$\sigma$	Standard deviation
$\gamma$	Gas gravity

$\rho_{(y)}$	Local density
$\mu_{(y)}$	Local viscosity
$\rho_{3-p}$	Three-phase homogeneous density
$\mu_{3-p}$	Three-phase homogeneous viscosity
$\alpha$	Void fraction
$\varphi$	Volumetric concentration
$\nu$	Kinematic viscosity

## **Introduction and Overview**

Hydrate formation and plugging is considered to be one of the most challenging flow assurance problems faced in the offshore oil and gas industry [Sloan 1998]. Moreover, pipelines carrying natural gas are more susceptible to burst and explosion as a result of hydrate plugging. The oil and gas industry spends up to 8% of their total estimated operating cost for the remediation of hydrates where hydrate inhibition costs are estimated at 220 million dollars annually (Sloan, 2003). Furthermore, significant amount of money (Lederhos, Long, Sum, Christiansen, & Sloan Jr, 1996) is spent annually on research to study the phenomena: hydrate formation and prevention strategies.

There are extensive studies carried out on hydrate formation and several conceptual models have been developed to understand the nucleation of hydrates. However, the assessment of hydrate formation probability and their associated risks are still in their infancy. Therefore, it is of great importance to evaluate and predict the probability of hydrate formation for any given operating condition, which enables any blockages or other associated incidents/accidents due to hydrate formation to be prevented. In this study, a novel methodology is developed to assess the probability of hydrate formation and the associated risks. Furthermore, a risk-based approach is presented to determine the parameters of winterization schemes as prevention strategies for hydrate formation for natural gas pipelines operating in Arctic conditions.

Objective of the present work are based on:

- To develop a method to quantify the likelihood of reaching hydrate forming conditions in probabilistic terms
- To develop a method to estimate the probability of hydrate formation and associated risks for natural gas pipelines operating in Arctic conditions
- To determine the parameters of winterization schemes to prevent hydrate formation using a risk-based winterization approach
- To test the applicability of a combined winterization approach to prevent hydrate formation

This thesis is written in manuscript format and is divided into five main chapters including the introduction and overview and Summary (Chapter 5). The following paragraphs briefly outline the chapters.

Chapter 1 describes the natural phenomena of hydrate formation including the characteristics of hydrates, typical hydrate forming conditions in oil and gas industry, hydrate prevention strategies and literature on calculation methods of hydrate forming conditions.

Chapter 2 is on development of a novel methodology to assess the probability of hydrate formation in a subsea production and transportation system, for a given operating condition and composition. The proposed method quantifies the likelihood of reaching hydrate-stable zone in probabilistic terms by adopting Shortest Path of Hydrate Formation (SPHF) which considers all achievable pathways for any given operating point (temperature and pressure) to reach hydrate forming conditions. Validation of the method is carried out through

obtaining a relationship between the probability curves developed for the two scenarios: with and without inhibition. This paper is published in Journal of Petroleum Science and Engineering (Herath, Khan, Rathnayaka, & Rahman, 2015).

Chapter 3 presents details of a novel risk-based methodology to calculate the parameters of winterization for pipelines operating in Arctic conditions to avoid hydrate formation. The applicability and effectiveness of a combined winterization strategy are demonstrated through examples. This paper is submitted to the Journal of Ocean Engineering.

In Chapter 4, a multiphase lab-scale flow loop set-up is proposed to study the effects of pipe diameter, wall roughness, solid particles and hydrodynamic properties on hydrate formation. A comprehensive analysis is carried out on the multiphase development length of a pipe for varying geometric and flow parameters to assist in identifying accurate development length for gas/liquid/solid multiphase flow. Also, some suggestions for future work are provided. This paper is published in the proceedings of ASME 2015 34<sup>th</sup> International Conference on Ocean, Offshore and Arctic Engineering (Herath, Rathnayaka, Rahman, & Khan, 2015).

Chapter 5 is the summary of the thesis and presents recommendations for future work.

## **Co-authorship Statement**

In all the papers presented in the following chapters, myself, Dinesh Bandara Herath, is the principle author and my supervisor Dr. Faisal Khan provided theoretical and technical guidance, support with analysis, reviewing and revising of the manuscripts. I have carried out most of the data collection and analysis. I have prepared the first drafts of the manuscripts and subsequently revised the manuscripts based on the co-authors' feedback and the peer review process. Co-author and supervisor Dr. Faisal Khan assisted in developing the concepts and testing of the models. As co-authors, Samith Rathnayake, Dr. Aziz Rahman and Dr. Ming Yang contributed through support in development of models, reviewing and revising the manuscripts.

## **Chapter 1. Hydrate Formation**

The increasing demand for energy has moved the oil and gas industry to the extremes by increasing explorations in deep water and the Arctic. This has significantly increased the risk of flow assurance problems. Flow assurance involves handling of solid deposits from hydrocarbon fluids in oil and gas flow lines where gas hydrates, corrosion, wax and slugging are a few of the common flow assurance problems. Hydrate formation is considered to be the prime flow assurance problem in offshore oil and gas industry (Davies et al., 2008) among the aforementioned flow assurance risks. In this chapter the focus is on review on fundamental mechanisms of hydrate formation, hydrate forming conditions with a focus on different calculation methods including both simple calculations and computer assisted calculation methods, hydrate formation in subsea equipment and hydrate prevention strategies.

### **1.1 Hydrates**

Hydrates, also more commonly known as Clathrates, are soli-crystalline compounds which are composed of water and light gas molecules. Since natural gas hydrates are composed of approximately 83 mol% of water, many physical properties of hydrates are similar to that of ice. But hydrates have different die-electric constant and thermal conductivity than that of ice. Due to the presence of gas molecules, hydrates exist at higher temperatures than ice.

Hydrates are formed when light hydrocarbons and water are present under certain temperature and pressure conditions, generally low temperatures and corresponding high

pressures. These conditions are more likely to occur during transient operating conditions such as, in the event of shutdown or restart operation of the wellhead and Christmas tree. For instance; the shutdown of a well will cause the temperature of subsea equipment to drop to the temperature of the surrounding where hydrates tend to form, given high pressure conditions. However, for pipelines operating in Arctic conditions, ambient temperature is the dominant factor for hydrate formation due to the extreme cold weather conditions.

Flow conditions below the downhole safety valve are typically unfavorable for hydrate formation, since hydrocarbon fluids are at higher temperatures (greater than the Hydrate Equilibrium temperature (HET) corresponding to the local pressure). Also, it is unlikely to form hydrates under steady state conditions, where the temperature of hydrocarbon mixture is higher, exceeding HET. Nevertheless, there is a high tendency of hydrate formation across subsea valves in deepwater oil production due to the phenomena of Joules-Thomson cooling, where hydrates are formed due to the rapid gas cooling by Joules-Thomson expansion. The rapid expansion of gas through a valve results in rapid cooling of fluid (faster than heat transfer) creating the conditions which allows the system to enter the hydrate stable regime.

## **1.2 Hydrate forming conditions**

Hydrates are solid crystalline compounds, formed when water come into contact with light hydrocarbon gases, usually under high pressure and low temperature. Typically four conditions are necessary for the forming of hydrates as shown in Figure 1-1.

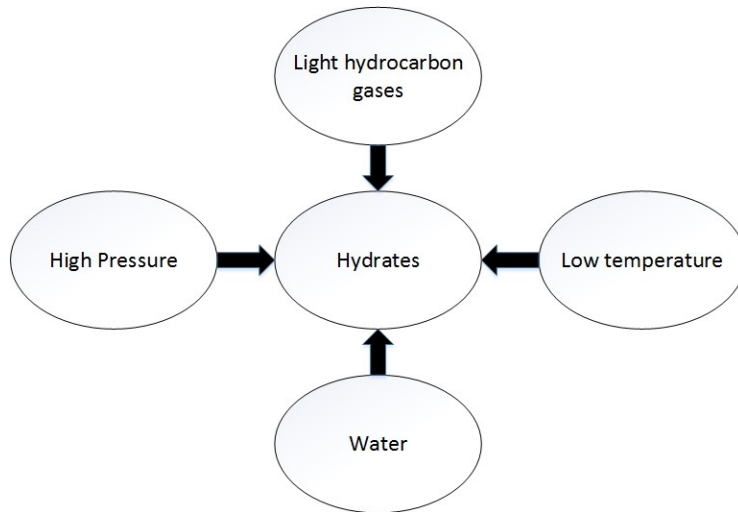


Figure 1-1: Hydrate forming conditions

Hydrate formation and dissociation curves represent the relationship between temperature and pressure conditions for the stability of natural gas hydrates. Figure 1-2 shows typical hydrate forming curves for different inhibition levels. To the right of the hydrate forming curve is the hydrate free region (where hydrates do not form) and to the left of the hydrate forming curve is the hydrate stable region (where hydrates tend to form).

As shown in Figure 1-2, the hydrate forming curves represent the temperature and pressure conditions at which hydrates form. However, this does not mean that hydrates will necessarily form and cause flow assurance problems even if the temperature and pressure conditions of the hydrocarbon system (with the presence of water) is close to the hydrate dissociation curve. For the nucleation of hydrates to occur, a certain amount of subcooling and delay time (induction time) is required. Generally, the time required for hydrate formation decreases exponentially with the increase of subcooling. Subcooling is defined as the temperature difference between hydrate stability temperature and the operating

temperature (at the same pressure). Generally, hydrate nucleation tends to occur at subcooling temperatures greater than 5°F (Bai & Bai, 2005).

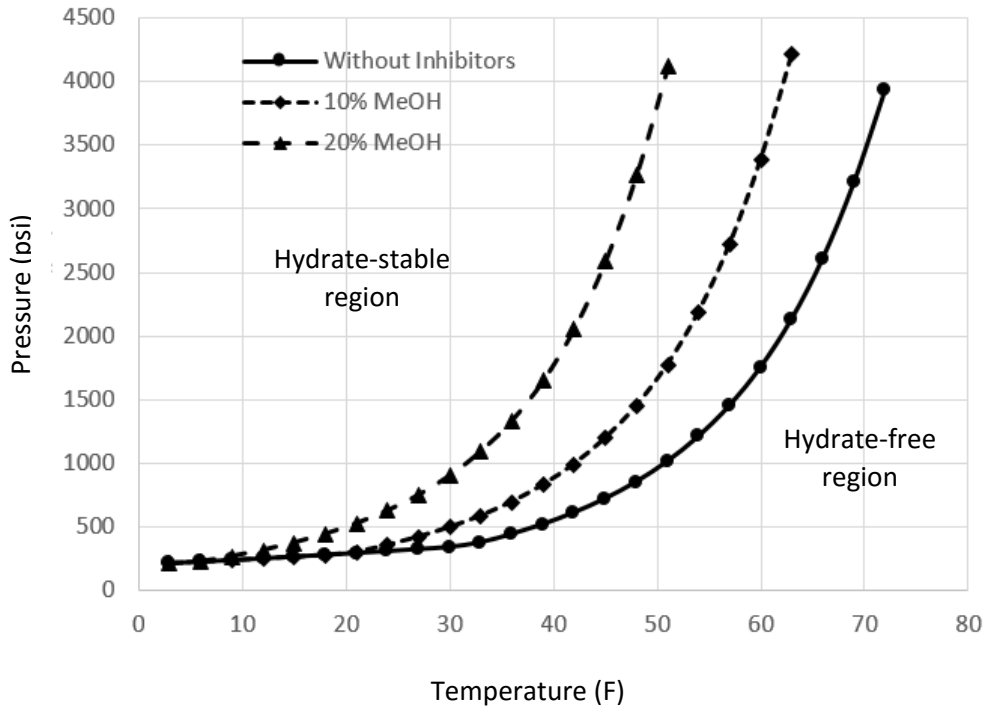


Figure 1-2: Hydrate forming curves for different inhibition levels

### 1.3 Types of Hydrates

Hydrate crystals have complex, 3-D structures in which the water molecules (host) form a cage and hydrate formers (guest) become entrapped in the cages. The crystalline structure is composed of polyhedral cages of hydrogen-bonded water molecules. These cages are stabilized by Van der Waals forces between the water molecules and the enclathrated guest molecule. There are three main hydrate crystal lattice structures which are classified by the arrangement of water molecules in the crystal (Carroll, 2009):

- Structure I: forms with small and middle sized natural gas molecules. Common type I hydrate formers include methane, ethane, carbon dioxide and hydrogen sulfide
- Structure II: a diamond lattice within a cubic framework which forms in the presence of gases or oils containing molecules larger than ethane and smaller than pentane. Common type II hydrate formers include nitrogen, propane and isobutane
- H- Structure: a hexagonal structure which consists of cavities large enough to contain large molecules. Common type H hydrate formers include 2-methylbutane, 2,3-dimethylbutane, 2,2,3-trimethylbutane, methylcyclopentane etc.

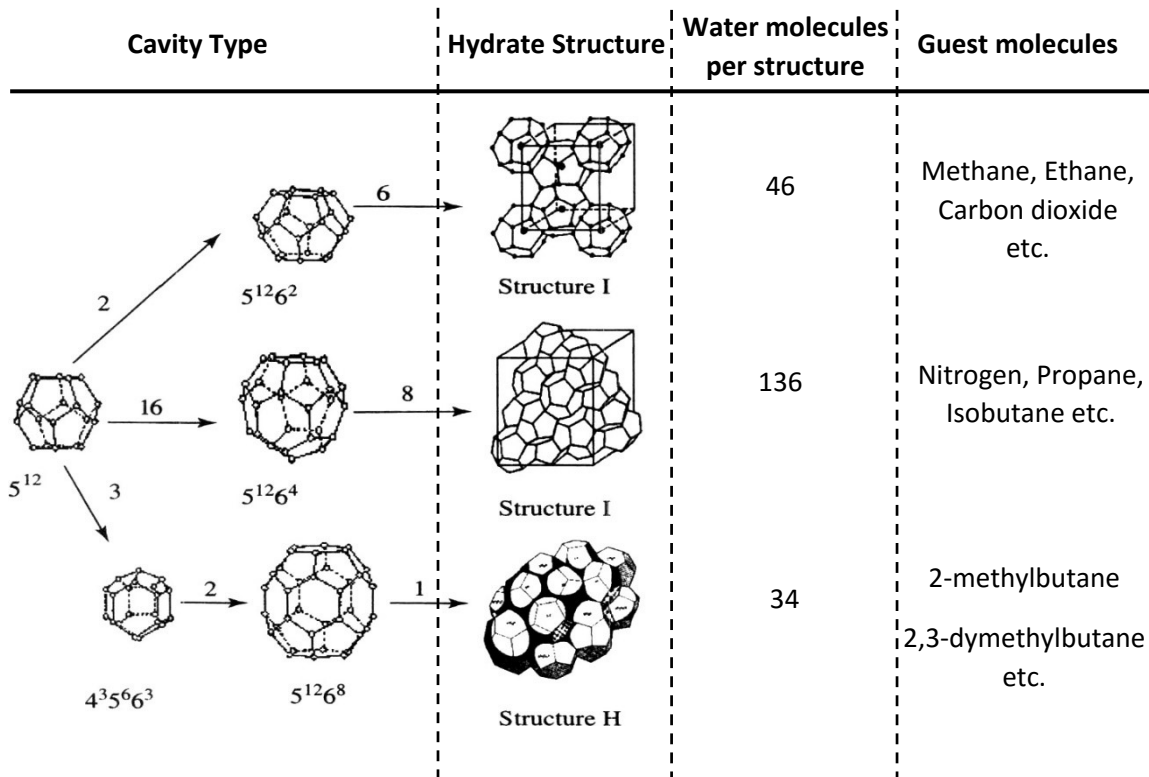


Figure 1-3: Hydrate structures

Structure I and II are the most commonly experienced lattice structures whereas the more complex H- Structure is not often encountered. Figure 1-3 shows the three common hydrate structures (Letcher, 2004). Pentagonal dodecahedra ( $5^{12}$ ) is the basic building block for the structures I and II, which has 12 faces of pentagonally bonded water molecules. In the crystal structure  $5^x6^y$ , x and y denotes the pentagonal and hexagonal sides in a cavity respectively.

#### 1.4 Indications of hydrate formations in pipelines under different operating conditions

It is of topmost importance to recognize any signs that point to hydrate formation in pipelines under varying operating conditions. This enables to take necessary preliminary actions to avoid any losses. Figure 1-4 shows different operating conditions and deviations from normal operations to identify hydrate formation in pipelines.

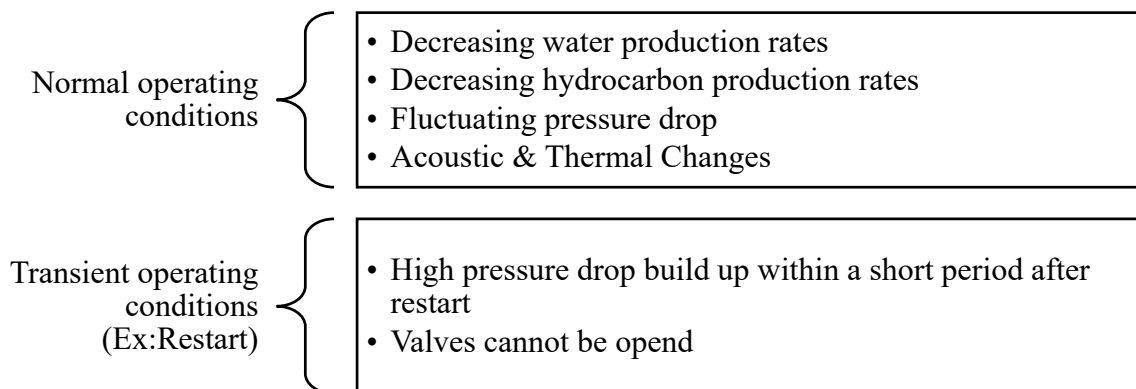


Figure 1-4: Different operating conditions where hydrates tend to form

## 1.5 Hydrate formation in Subsea Safety Equipment

Hydrate plugs tend to form in subsea equipment due to favorable hydrate forming conditions. Generally, transient conditions such as start-up, shutdown or restart are susceptible to hydrate forming. For instance, the shutdown of a well will cause the temperature of subsea equipment to drop to the temperature of surrounding where hydrates tend to form at given high pressure conditions. It is unlikely to form hydrates under steady state conditions where temperature of hydrocarbon fluids is higher, exceeding Hydrate Equilibrium Temperature (HET).

In Gulf of Mexico where many deepwater oil and gas explorations are ongoing, the temperature at sea bed is constant at approximately 40°F (deeper than 300ft). Therefore during transient operations (shut-in, start-up) the risk of hydrate formation at subsea equipment (SSV, Choke valve) is high where the ambient temperatures are typically around 40 °F.

There is a high tendency of hydrate formation across subsea valves in deepwater oil production due to the phenomena of Joules-Thomson cooling, where hydrates are formed due to the rapid gas cooling due to the isenthalpic process of Joule-Thomson expansion. The rapid expansion of gas through a valve results in rapid cooling of fluid (faster than heat transfer) creating the conditions which allows the system to enter the hydrate formation regime. Therefore, in transient well operations such as start-up and well-testing, hydrates may form at downstream of valves with high pressure drops. Hydrates may form even with a high initial temperature due to the rapid temperature drop through valves. Katz (Katz,

1945) has developed constant enthalpy (isenthalpic) charts for gases with several gas gravities (0.6-0.8), specifying the lowest downstream pressure (without hydrate formation) given the upstream temperature and pressure (Figure 1-5).

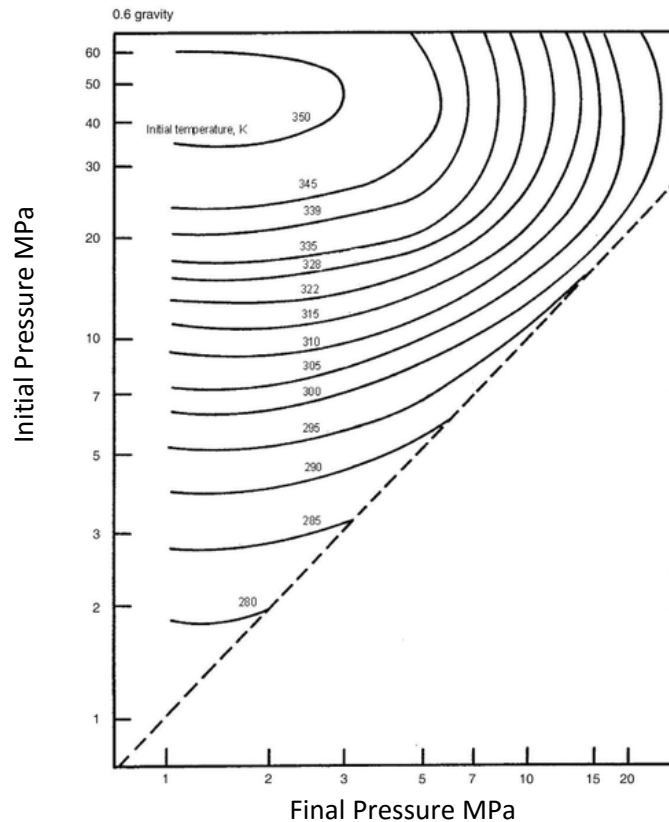


Figure 1-5: Permissible expansion of a 0.6 gravity natural gas without hydrate formation (Katz, 1945)

Due to the high temperature of hydrocarbon fluids below the downhole safety valve, hydrate formation is unlikely.

In a gas production system, a choke valve is mandatory for the control of gas flow rates. The choking process causes a pressure drop across the valve which in turn causes a decrease in gas temperature, leading to an increase in the risk of hydrate formation.

## 1.6 Hydrate prevention

In order to prevent hydrate formation, any one of the key factors contributing for hydrate formation (Figure 1-1) should be avoided. Current methods for hydrate prevention are generally based on one or the combination of the following techniques;

- Removal of water (both free and dissolved) from the system: which could be achieved either by molecular sieves to lower water content or using triethylene glycol.
- Injecting chemical/thermodynamic inhibitors: Salts, Alcohols, Glycols
- Injecting kinetic inhibitors into the water phase.
- Adding anti-agglomerants
- Maintaining high temperatures: by means of insulation and/or heating, which keeps the system in the hydrate free region
- Re-modifying the piping system to avoid low points, restrictions etc.

Removal of water is considered to be the most reliable amongst all preventive methods stated above. But water removal may not be viable due to remote locations and submersion. Hence, inhibition is the most common hydrate prevention strategy adapted by the oil and gas industry where millions of dollars are spent on inhibition annually (Sloan, 2003). Flow channels are frequently operated with inhibitor injection at the well followed by dehydration at a downstream point. Inhibitors are injected into the gas stream either using chemical injection pumps or drips. The more frequently used inhibitors are strong polar fluids, such as methanol, the ethylene glycols, and ammonia. Methanol/glycol injection

systems tie up free water and water vapour to prevent hydrate formation. Methanol is often preferred over glycol due to economic reasons. Though methanol is cheaper than glycol on a volume basis, it cannot be recovered and regenerated. Whereas glycol can be recovered and regenerated for reuse easily. Hence, in gas dominated systems, MEG is preferred over MeOH due to recovery. Another advantage of glycol over methanol is the low injection rates.

The addition of inhibitors shifts the hydrate equilibrium curve towards lower temperatures, minimizing the risk of hydrate formation by reducing the temperature or increasing the pressure at which hydrates form. The formula proposed by Hammerschmidt (1934) is still widely being used in the natural gas industry to approximate the temperature depression due to inhibition.

$$\Delta T = \frac{K_H W}{M(100 - W)} \quad (1-1)$$

Where  $\Delta T$  ( $^{\circ}\text{C}$ ) is the temperature depression due to inhibition,  $W$  (%w.t.) is the concentration of the inhibitor in weight percent in the aqueous phase,  $M$  (g/mol) is the molar mass of inhibitor and  $K_H$  is a constant (for MeOH: 1297). A revised version of Hammerschmidt equation was proposed by Nielsen and Bucklin (1983) for the use of methanol injection systems.

$$\Delta T = -129.6 \ln(1 - x_{\text{MeOH}}) \quad (1-2)$$

Where  $\Delta T$  is the temperature depression due to inhibition ( $^{\circ}\text{F}$ ) and  $x_{\text{MeOH}}$  is the mole fraction of inhibitor in liquid phase.

## 1.7 Predicting hydrate forming conditions

Statistical thermodynamics using van der Waals and Platteeuw model with alterations can be effectively used to predict hydrate forming conditions (Sloan, 1998). However, hydrate forming conditions can also be calculated by simple and straight forward phase diagrams and correlations based on gas gravity. Research work has been carried out extensively in the area of hydrate formation and in deducing hydrate formation conditions, through laboratory experiments. In a study conducted using pure Methane (Gudmundsson, Parlaktuna, & Khokhar, 1994), through laboratory experiments it was deduced that the pressure and temperature requirements for hydrate formation as 290-870 psi and 32-68°F. In another study, Rajnauth et. al (Rajnauth, Barrufet, & Falcone, 2012) revealed that the compositions of natural gas affects the temperature and pressure requirements for hydrate formation, through a sensitivity analysis. Furthermore, the results of their study showed that the presence of impurities (Carbon Dioxide, Nitrogen and Hydrogen Sulfide) in natural gas has a significant impact on the hydrate formation conditions.

Sun et al. (2010) compared the two thermodynamic models; van der Waal Platteeuw model and Chen-Guo model to analyze hydrate formation with high CO<sub>2</sub> content using both experimental data and values predicted by the models. A significant increase in hydrate formation was observed in experiments for increasing pressures at constant temperature. Also, the Vander-waals and Chen Guo models deviated largely from experimental results. There are different methods available to calculate hydrate forming conditions as outlined in the following sections.

## **1.8 K-factor method**

The K-factor method or the  $K_i$  method is one of the earliest hand calculation methods proposed by Carson and Katz to estimate hydrate forming conditions for gas mixtures (Carson & Katz, 1942).  $K_i$  is defined as the component distribution between the hydrate and the gas (mole fraction of the component divided by that of the hydrate). These  $K_i$  values are used to obtain hydrate dew-point for a gas with constant composition.

### **1.8.1 Gas gravity method**

A more compact and simple method of quantifying hydrate formation conditions (Pressure and Temperature) is the gas gravity method which could be used as a first estimate in hand calculations. In this method, once the gas gravity and the lowest temperature of the process is specified, the hydrate forming pressure could be read from the chart shown in Figure 1-6 (Katz, 1945).

### **1.8.2 Correlations based on gas gravity method**

There are many correlations based on gas gravity method developed by researchers to estimate the hydrate forming conditions. These methods are not highly accurate, but can be used effectively in spreadsheet calculations as an approximate method. However correlations based on gas gravity method are not recommended to calculate hydrate forming conditions of sweet natural gas mixtures (Carroll, 2009). Three of the commonly used correlations are given below;

Towler-Mokhatab (Mokhatab & Towler, 2005);

$$T = 13.47 \ln(P) + 34.27 \ln(\gamma) - 1.675 \ln(P) \ln(\gamma) - 20.35 \quad (1-3)$$

Motiee (Motiee, 1991);

$$T = -283.24469 + 78.99667 \log(P) - 5.352544 \log(P)^2 \quad (1-4)$$

$$+ 349.473877\gamma - 150.854675\gamma^2 - 27.604065 \log(P) \gamma$$

Where  $\gamma$  is the gas gravity of the mixture.

Makogon;

$$\log P = \beta + 0.0497(t + kt^2) - 1 \quad (1-5)$$

Graphical correlations were provided for  $\beta$  and  $k$ .

Though hand calculation methods are still being used as approximations, with the advancement of computer technology, many software packages with the capability of hydrate calculations have been developed such as: PVTsim, PIPESIM and Hysys. These computer-based software packages are built on rigorous thermodynamic models and are more accurate than hand calculation methods. There are tools which are dedicated for hydrate calculations such as CSMHYD (Sloan, 1998) developed by Colorado School of Mines. Also, a transient gas hydrate model- CSMHyK, has been designed to predict formation and transportability of gas hydrates in oil-dominated flow lines, by the Centre for Hydrate Research: Colorado School of Mines (Zerpa, Sloan, Sum, & Koh, 2012).

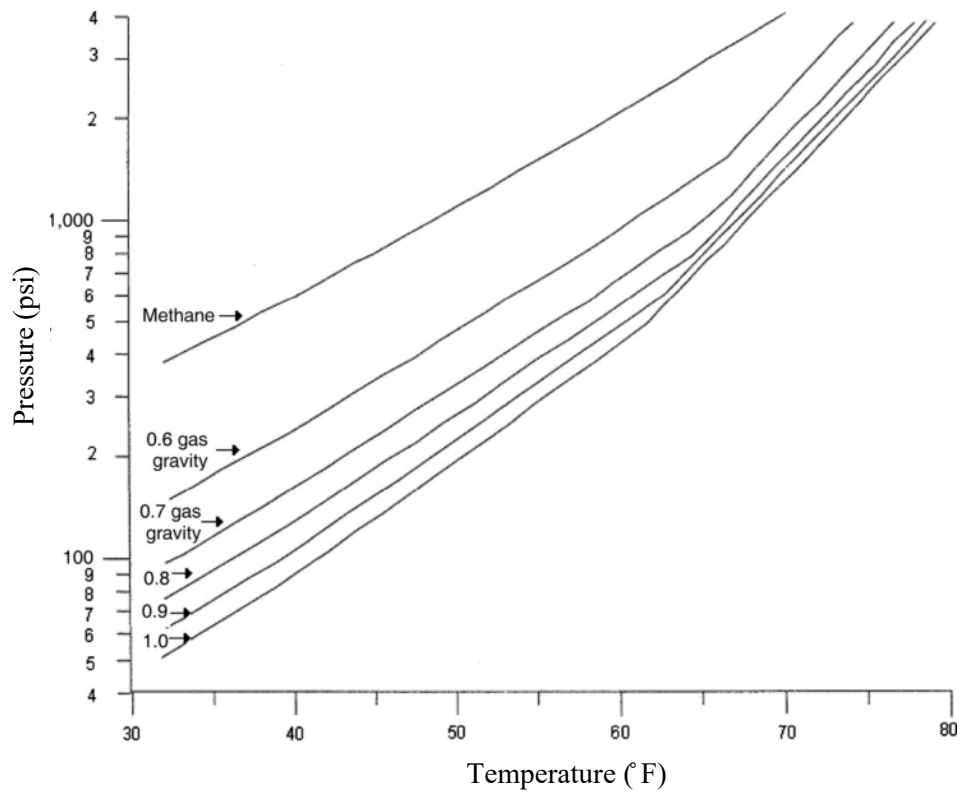


Figure 1-6: Pressure-Temperature curves for predicting hydrate formation (Katz, 1945)

## 1.9 References

- Bai, Y., & Bai, Q. (2005). *Subsea Pipelines and Risers*. Elsevier.
- Carroll, J. (2009). *Natural Gas Hydrates: A Guide for Engineers*. Gulf Professional Publishing.
- Carson, D. B., & Katz, D. L. (1942). Natural Gas Hydrates. *Transactions of the AIME*, 146(01), 150–158. <http://doi.org/10.2118/942150-G>
- Davies, S. R., Boxall, J., Koh, C. A., Sloan, E. D., Hemmingsen, P., Kinnari, K. J., & Xu, Z.-G. (2008). Predicting Hydrate Plug Formation in a Subsea Tieback. Society of Petroleum Engineers. <http://doi.org/10.2118/115763-MS>
- Gudmundsson, J.-S., Parlaktuna, M., & Khokhar, A. A. (1994). Storage of Natural Gas as Frozen Hydrate. *SPE Production & Facilities*, 9(01), 69–73. <http://doi.org/10.2118/24924-PA>
- Hammerschmidt, E. G. (1934). Formation of Gas Hydrates in Natural Gas Transmission Lines. *Industrial & Engineering Chemistry*, 26(8), 851–855. <http://doi.org/10.1021/ie50296a010>
- Herath, D., Khan, F., Rathnayaka, S., & Rahman, M. A. (2015). Probabilistic estimation of hydrate formation. *Journal of Petroleum Science and Engineering*, 135, 32–38. <http://doi.org/10.1016/j.petrol.2015.08.007>
- Herath, D., Rathnayaka, S., Rahman, M. A., & Khan, F. (2015). Multiphase Hydrate Induction Experiment in a Subsea Pipeline, V010T11A021. <http://doi.org/10.1115/OMAE2015-41602>

- Katz, D. L. (1945). Prediction of Conditions for Hydrate Formation in Natural Gases. *Transactions of the AIME*, 160(01), 140–149. <http://doi.org/10.2118/945140-G>
- Lederhos, J. P., Long, J. P., Sum, A., Christiansen, R. L., & Sloan Jr, E. D. (1996). Effective kinetic inhibitors for natural gas hydrates. *Chemical Engineering Science*, 51(8), 1221–1229. [http://doi.org/10.1016/0009-2509\(95\)00370-3](http://doi.org/10.1016/0009-2509(95)00370-3)
- Letcher, T. (2004). *Chemical Thermodynamics for Industry: RSC* (1 edition). Cambridge, U.K: Royal Society of Chemistry.
- Mokhatab, S., & Towler, B. (2005). Quickly estimate hydrate formation conditions in natural gases. *Hydrocarbon Processing*, 61–2.
- Motiee, M. (1991). Estimate Possibility of Hydrates. *Hydrocarbon Processing*, 70(7), 98–99.
- Nielsen, R. B., & Bucklin, R. W. (1983). Why Not Use Methanol for Hydrate Control? *Hydrocarbon Processing*, 62(4), 71.
- Rajnauth, J., Barrufet, M., & Falcone, G. (2012). Hydrate Formation: Considering the effects of Pressure, Temperature, Composition and Water. *Energy Science and Technology*, 4(1), 60–67. <http://doi.org/10.3968/j.est.1923847920120401.397>
- Sloan, E. D. (1998). *Clathrate Hydrates of Natural Gases, Second Edition, Revised and Expanded*. CRC Press.
- Sloan, E. D. (2003). Fundamental principles and applications of natural gas hydrates. *Nature*, 426(6964), 353–363. <http://doi.org/10.1038/nature02135>
- Sun, R., Li, C., Yu, S., Wang, S., Sun, O., & Liu, E. (2010). Hydrate Formation Conditions of Natural Gas with High Content of Carbon Dioxide and the

Calculation Model. Society of Petroleum Engineers.

<http://doi.org/10.2118/131812-MS>

Zerpa, L. E., Sloan, E. D., Sum, A. K., & Koh, C. A. (2012). Overview of CSMHyK: A transient hydrate formation model. *Journal of Petroleum Science and Engineering*, 98–99, 122–129. <http://doi.org/10.1016/j.petrol.2012.08.017>

## Chapter 2. Probabilistic Estimation of Hydrate Formation

Dinesh Herath, Faisal Khan, Samith Rathnayaka, Aziz Rahman

*Safety and Risk Engineering Group (SREG), Faculty of Engineering and Applied  
Science, Memorial University of Newfoundland, St. John's, NL, Canada*

### Abstract

Hydrate formation is one of the major challenges for offshore oil and gas production and the transportation industry. The blockage of subsea pipelines and equipment due to hydrate formation imposes a potential safety hazard. To ensure continuous functionality of the production system and minimize production losses, many approaches are currently being adopted by the industry where probabilistic estimation of hydrate formation can be considered as a critical step of safety evaluation. In this work, a novel approach is proposed to predict hydrate formation probability in a subsea production and transportation system for a given composition and operating conditions. The proposed approach considers the Shortest Path of Hydrate Formation (SPHF) in predicting the probability of hydrate formation.

Keywords: Offshore, Safety, Probability, Hydrate, Shortest Path of Hydrate Formation (SPHF).

### Nomenclature

$T_{SP}$  = Temperature at safe point, °F

$P_{SP}$  = Pressure at safe point, psi

$T_i$  = Temperature at intersecting point, °F

$P_i$  = Pressure at intersecting point, psi

$T_{OP}$  = Temperature at operating point, °F

$P_{OP}$  = Pressure at operating point, psi

$T_{md}$  = Mean difference between safe temperature and average temperature on hydrate equilibrium curve, °F

$P_{md}$  = Mean difference between safe pressure and average pressure on hydrate equilibrium curve, psi

$\Delta T$  = Temperature depression due to inhibition, °F

$x_{MeOH}$  = Mole fraction of inhibitor in liquid phase, wt%

## 2.1 Introduction

With the ever rising demand for energy, offshore drilling continues to be pushed to new depths, increasing the exploration for oil and gas resources in deeper and farther offshore sites. The continuous drilling in deepsea with depths over 5,000 feet poses higher risks due to catastrophic accidents, spills and fires. This requires rigorous risk assessment related to hydrate formation ensuring safer design and equipment integrity. Formation of hydrates is considered to be one of the many challenges faced in deepsea operations where hydrate formation may result in blockage of subsea pipelines and equipment (Sloan, 1998). Hydrate plugging is the prime problem in offshore flow assurance compared to other flow assurance challenges, such as solids asphaltenes or waxes (Davies et al., 2008). Pipelines carrying

natural gas are more susceptible to burst and explosion as a result of hydrate plugging. During dissociation of hydrates in a pipeline, any pressure gradient across a plug will result in hydrates travelling at very high velocities and compress downstream gas which causes blowouts (Sloan, 2003). To restrain the formation of hydrates in subsea equipment, the oil and gas industry spends up to 8% of their total estimated operating cost. Hydrate inhibition costs are estimated at 220 million dollars annually (Sloan, 2003).

In order to mitigate economic risks in the offshore oil and gas industry, a significant amount of money (Lederhos, Long, Sum, Christiansen, & Sloan Jr, 1996) is spent annually on research to study the phenomena of hydrate formation and prevention. Among the various methods available for preventing hydrate formation in pipelines (insulation, heating and inhibition), the use of kinematic inhibitors is widely adopted. Understanding of hydrate formation and prevention methods are under constant research (Seo & Kang, 2012; Urdahl, Børnes, Kinnari, & Holme, 2004; M. Wu, Wang, & Liu, 2007). Research related to hydrates has been carried out extensively during the past two decades to better understand and hinder this undesirable phenomena. Several conceptual models are available which have been developed to describe the nucleation of hydrates. Colorado School of Mines Hydrate Kinetics (CSMHyK) model is a gas hydrate model specifically designed for oil-dominated systems based on the conceptual model which assumes that hydrates form at the interface of water droplets and continuous oil phase (Zerpa, Sloan, Sum, & Koh, 2012). Several methods are available to predict hydrate forming pressure and temperature, out of which the K-factor (Carson & Katz, 1942) method is most frequently referred to in literature. There are other correlations developed by researchers to estimate hydrate

forming conditions based on gas gravity such as Elgibaly and Elkamel (1998), Towler and Mokhatab (2005), Motiee (1991) and so on. Most of the commercially available process simulation software (PVTsim, PIPESIM, Hysys etc.) has the capability of predicting hydrate forming conditions. However, there are other tools dedicated to hydrate calculations such as *CSMHYD* (Sloan, 1998). Though general phase equilibrium calculations are performed using fugacities, hydrate calculations are based on chemical potentials where the hydrate formation process is modelled in two steps (with a hypothetical state for the ease of calculations). Carrol (2009) explains both hand calculation methods as well as computer methods in detail. Induction time in gas hydrate crystallization plays a vital role in hydrate research due to its association with kinetic inhibitors, where both induction time and growth/agglomeration of hydrate crystals are affected by kinetic inhibitors (Kashchiev & Firoozabadi, 2003). Different models for calculating induction time can be found in literature (Kashchiev, 2000).

Although several models have been developed regarding nucleation of hydrates, the assessment of hydrate formation probability and their associated risks are still in their infancy. Therefore, it is of great importance to evaluate and predict the probability of hydrate formation for any given operating condition, which enables any blockages or other associated incidents/accidents due to hydrate formation to be prevented. Deng et al. (2014) calculated the probability of hydrate formation using the combined probability method by establishing a “probability limit state equation” from the difference of hydrate formation temperature and operating temperature. They were able to calculate the probability of hydrate formation by adopting simulation methods for a temperature and pressure

distribution obtained from an experimental flow loop. This method entails the logging of temperature and pressure data for the generation of distributions and it is not capable of predicting the probability for a specific operating condition, which are considered as key limitations. Therefore, a better and rigorous method of predicting hydrate formation probability is required which assists in preventing hydrate blockage and subsequent equipment failure or catastrophic accidents.

This study mainly focuses on developing a novel methodology to assess the probability of hydrate formation for a given operating condition and composition. The present work is only focused on the right-hand side of the hydrate forming curve (hydrate-free zone) and develops a methodology to quantify the likelihood of reaching hydrate-stable zone in probabilistic terms. The proposed method considers all achievable pathways for any given operating point (temperature and pressure) to reach hydrate forming conditions. Due to the simplicity of proposed method, it does not require extensive logging of temperature and pressure data. Hence, the probability of hydrate formation of any natural gas pipeline with known composition and operating conditions can be easily predicted, expediting the decision making process around hydrate remediation. Furthermore, the present work can be considered as the first step towards the risk assessment of hydrate formation. To demonstrate the applicability of the proposed method, two case studies are considered. Also, two different scenarios with different compositions (99%-CH<sub>4</sub>, 1%-C<sub>2</sub>H<sub>6</sub> and 99%-CH<sub>4</sub>, 1%-C<sub>2</sub>H<sub>6</sub>, MeOH 10 wt%) are compared to validate the accuracy of the proposed methodology. Based on the findings, a novel correlation between the respective probability curves is presented.

## **2.2 Hydrate formation probability estimation method**

The proposed methodology can be summarized by four key steps as shown in Figure 2-1.

The four key steps are explained in detail in the following sections.

### **2.2.1 Calculation of hydrate forming conditions**

Hydrate forming curves are used to define the temperature and pressure conditions at which hydrates tend to form (Figure 2-2). In order to avoid the possibility of hydrate formation, the hydrocarbon system must operate outside the temperature and pressure envelope defined by the hydrate forming curve. Operating conditions to the left side of the hydrate formation curve fall into the hydrate-stable region while the right side of the curve is a hydrate-free region. The primary phase of the methodology involves generating a hydrate equilibrium curve where any of the aforementioned (Section 2.1) commercially available software can be utilized. Then the corresponding hydrate forming pressure and temperature data are imported into *Matlab* code. For the formulation of probability equations it is required to fit the hydrate equilibrium curve into a polynomial function, which will assist in developing relations between pressure and temperature conditions where hydrates form. Depending on the level of accuracy required, higher order polynomial functions can be used.

Once the hydrate curve is generated, all the reference values such as average reservoir pressure, ambient temperature (of deepsea), and the pressure and temperature values at the safe point are defined for the specific scenario considered. Deep subsea conditions are defined when water depth is greater than 3000ft and the temperature at seabed is around

39°F in all seasons (Bai & Bai, 2012). Therefore, for model development, it is reasonable to assume the average seawater temperature as the minimum temperature that can be reached by a gas producing pipeline in such harsh environmental conditions. Reservoir pressure of the considered offshore production system will be used as the maximum pressure in the pipeline.

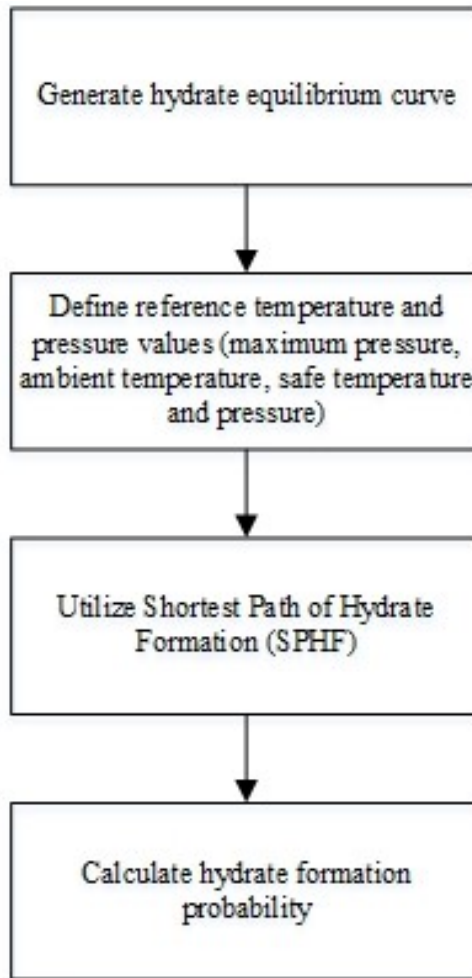


Figure 2-1: Methodology for the estimation of probability of hydrate formation

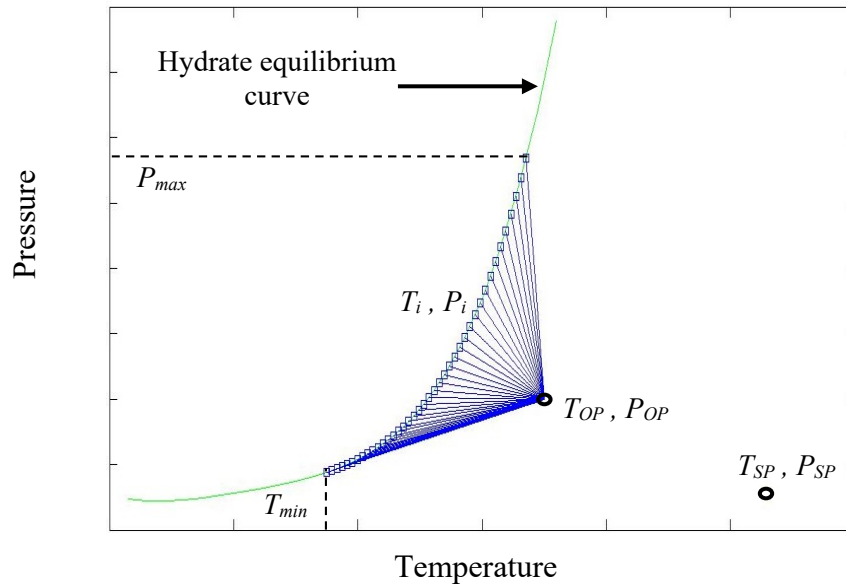


Figure 2-2: Possible shortest pathways

### 2.2.2 Shortest Path of Hydrate Formation (SPHF)

As presented in Figure 2-2, the hydrate formation curve (solid line) represents the temperature and pressure conditions at which hydrates form. Nevertheless this does not mean that hydrates will necessarily form and cause flow assurance problems since a certain amount of subcooling and delay time (induction time) are required for hydrates to transfer into a stable region (R. Wu et al., 2013). One of the main assumptions considered while developing the model is that hydrates form at the exact temperature and pressure conditions of the hydrate equilibrium curve. Though hydrates do not form at the right hand side of hydrate curve (hydrate-free zone), the changes in operating conditions along the pipeline due to various internal and external factors (e.g., temperature drop due to heat losses,

pressure losses due to friction and gravity) may bring the operating point inside the hydrate-stable region. This results in imposing a probability of hydrate formation for any operating point in the hydrate-free zone. The developed model considers the shortest distance between the point of release (operating point) and the equilibrium curve, hence straight lines. Therefore, for any given operating condition, the possible pathways of approaching the hydrate forming conditions (equilibrium curve) will span between the tangent lines generated from the operating point to the hydrate equilibrium curve. This represents all attainable temperature-pressure profiles along the pipe length under different heat and pressure losses. Though in reality the temperature-pressure profile along the pipe length is not always linear, it is assumed to be linear to simplify the model development. Moreover, the system cannot reach temperature values less than the specified minimum (i.e., average seawater temperature) and pressure values above the specified maximum (i.e., reservoir pressure). Therefore, if the temperature and pressure values of the two intersecting points of the tangent lines and equilibrium curve exceed the aforementioned limitations, the minimum achievable temperature and the maximum achievable pressure should be considered as the points which define the range of pathways. Figure 2-3 summarizes the method for obtaining pathways through which the operating point reaches hydrate forming conditions.

### **2.2.3 Definition of safe temperature and pressure**

For natural gas transmission lines, operation at higher pressure and lower temperature promotes rapid hydrate formation (Sloan, 2005). Therefore, as a rule of thumb it is reasonable to assume that a high temperature and low pressure condition represents a

hydrate-free region. The safe temperature and pressure can be considered as the operating conditions without any hydrate threat. Hence any point which has a significant difference from hydrate forming temperature and pressure conditions can be considered as a safe point. The values for safe temperature and pressure vary with the system as they depend on multiple factors such as gas composition, operating conditions and environmental loads. The mean temperature difference between the safe point and points on the hydrate equilibrium curve ( $T_{md}$ ) is used to define the basis of obtaining the safe temperature ( $T_{SP}$ ) while the mean pressure between the safe point and points on the hydrate equilibrium curve ( $P_{md}$ ) is used to define the basis of obtaining the safe pressure ( $P_{SP}$ ).

$$\frac{\sum_{i=1}^n (T_{SP} - T_i)}{n} = T_{md} \quad (2-1)$$

$$\frac{\sum_{i=1}^n (P_i - P_{SP})}{n} = P_{md} \quad (2-2)$$

Since temperature and pressure conditions of the safe point depends on the hydrate equilibrium curve, each case with different compositions of gas and different inhibitor levels will have a unique safe temperature and pressure condition. It is also important to note that when obtaining safe temperature and pressure values, safe temperature should be always greater than the temperature corresponding to the maximum pressure and the safe pressure should be less than the pressure corresponding to the minimum temperature. An alternate and simplistic approach to obtain the safe temperature and pressure is to consider

the point with the maximum temperature and the pressure corresponding to the minimum temperature.

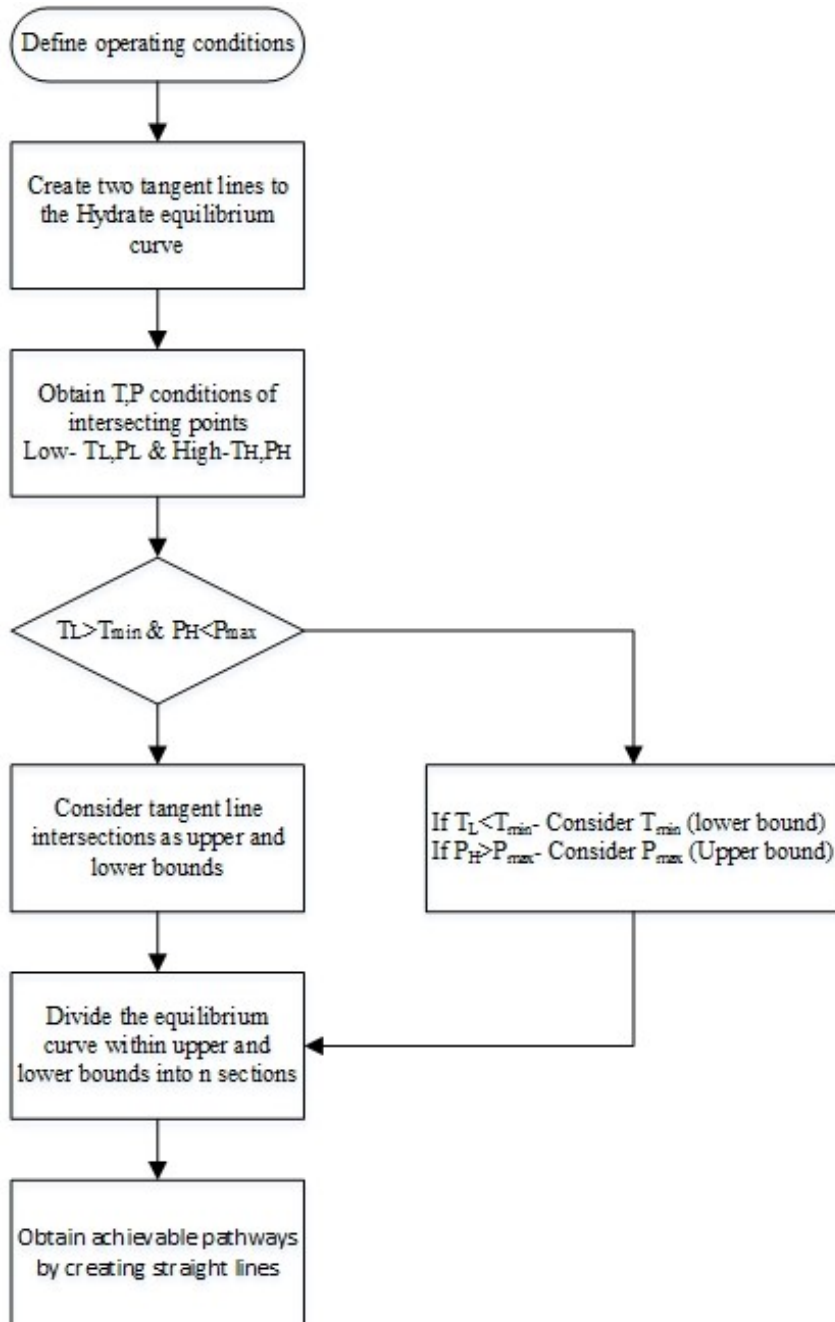


Figure 2-3: Algorithm to obtain achievable pathways using SPHF

### 2.3 Hydrate formation probability calculations

The ratio between a safe and a hazard value of any variable will provide a primary, but one of the most vital characteristic regarding the safety of any system. Similarly, in this case, temperature and pressure are considered as the deterministic parameters of safe and hazard values to obtain the probability of hydrate formation. If the equilibrium curve bounded by the two upper and lower intersecting lines is divided into n- number of segments, there are n+1 number of points at which the operating point can reach the hydrate forming conditions (along straight lines/pathways). Then, the probability of hydrate formation can be obtained in terms of pressure and temperature conditions at operating ( $T_{OP}, P_{OP}$ ), safe ( $T_{SP}, P_{SP}$ ) and intersecting points ( $T_i, P_i$ ) using the following equation (Eq.2-3).

$$Pr = \frac{1}{n} \sum_{i=1}^n \left( \frac{(T_{OP} - T_{SP})}{(T_i - T_{SP})} \right) * \left( \frac{(P_{OP} - P_{SP})}{(P_i - P_{SP})} \right) \quad (2-3)$$

As presented in Figure 2-4, the segment of the hydrate equilibrium curve within the range of possible pathways can be divided into three sections based on the T, P conditions of the failure point (point on equilibrium curve) and the operating point.

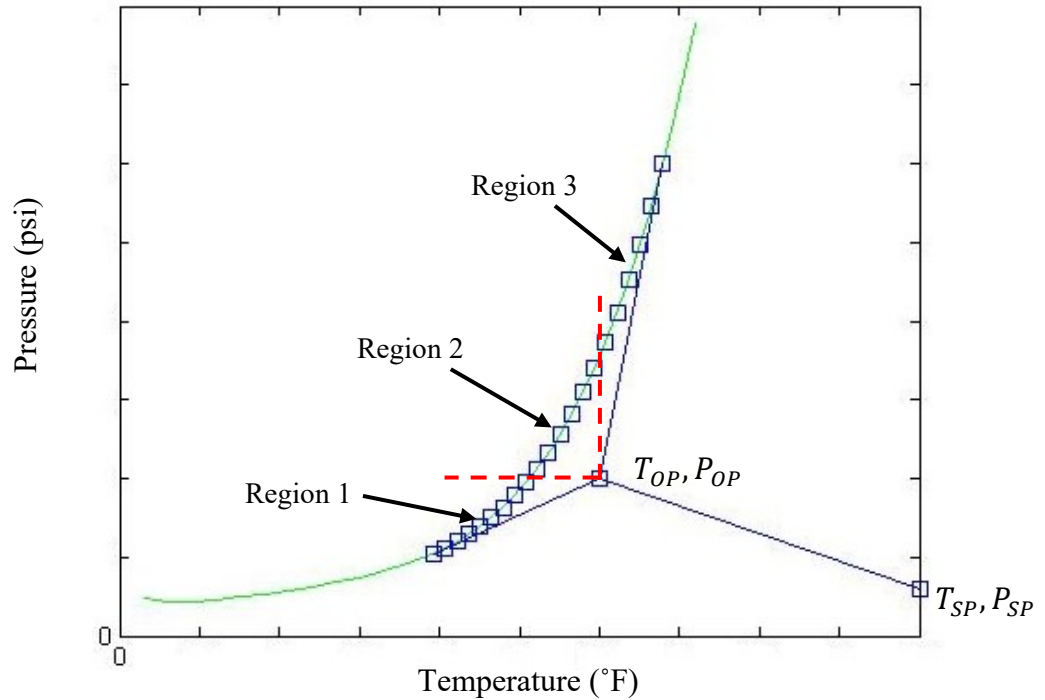


Figure 2-4: Calculation method

In region-1 in Figure 2-4, the hazard margin of pressure ( $P_{OP} - P_{SP}$ ) is greater than the safe margin of pressure ( $P_i - P_{SP}$ ), which allows the effect of pressure for hydrate formation to be considered 1 (the maximum). Similarly, from Figure 2-4, it is clearly observed that the operating temperature is less than the temperature values of the points on the hydrate curve for region-3. This will result in the operating temperature exceeding the safe margin with respect to safe temperature, which allows the effect of temperature for formation of hydrates to be maximum: 1. Therefore a more general form of equation is proposed as follows:

$$Pr_i = \begin{cases} \frac{(T_{OP} - T_{SP})}{(T_i - T_{SP})}; P_i \leq P_{OP} \\ \left( \frac{(T_{OP} - T_{SP})}{(T_i - T_{SP})} \right) * \left( \frac{(P_{OP} - P_{SP})}{(P_i - P_{SP})} \right); P_i > P_{OP}, T_i \leq T_{OP} \\ \frac{(P_{OP} - P_{SP})}{(P_i - P_{SP})}; T_i > T_{OP} \end{cases} \quad (2-4)$$

It is important to note that all the possible pathways through which the operating point can reach the hydrate forming conditions do not have the same likelihood, since the effects of heat losses and frictional losses dictate the temperature-pressure profile along the pipe length. In present work, for the ease of model development, all the possible pathways through which the operating point reach the hydrate forming conditions are considered to have the same likelihood.

Two case studies are considered in the following sections to demonstrate the applicability of the proposed method for the oil and gas industry.

### 2.3.1 Case Study I

In this study, a gas producing system which produces 99% methane (CH<sub>4</sub>) and 1% ethane (C<sub>2</sub>H<sub>6</sub>) is taken into consideration. Following the steps given from section 2.2-2.3, initially a hydrate equilibrium curve is generated for this composition using *PVTsim*. To adopt the aforementioned SPHF method, it is required to define values for the expected mean temperature and pressure differences. Considering a minimum temperature of 35°F (as described in Section 2.2.1) and a maximum pressure of 2500 psi, the mean temperature and pressure differences are assigned values of 50°F and 1000 psi respectfully. Using Eq.2-1

and Eq.2 (Section 2.3), conditions for the safe point are obtained (106 °F, 277.8 psi). Next, incorporating the attained values into *Matlab* code, the probability values for operating points lying in the total operating range are obtained and plotted in 2D figure as shown in Figure 2-5(a). To validate the accuracy of the proposed methodology (in Section 2.3), the same composition with 10 wt% methanol (MeOH) was considered and the probability values were plotted as shown in Figure 2-5(b). To better comprehend the change of probability of hydrate formation within the operating range, 2-D color plots are used. In both Figure 2-5(a) and Figure 2-5(b), the hydrate-stable region is represented by red color and hydrate-free region by blue color. In the presence of inhibition, the shift of the hydrate-stable region to lower temperatures and the increase of the low hydrate-probability region ( $<0.5$ ) are clearly visible.

Figure 2-6 shows the probability values obtained for different operating conditions within the area bounded by the temperature and pressure values of 35-106°F and 278-2300 psi, respectively. As presented in Figure 2-6, high pressure and low temperature regions display high probability values for hydrate formation, whereas low pressure and high temperature regions display low probabilities for hydrate formation which agrees with the proposed model of hydrate forming conditions. Moreover, it is important to note that for the case with inhibition (MeOH 10 wt%), for any fixed operating point the probability of hydrate formation is reduced, thus the effect of inhibition could be quantified in terms of probability.

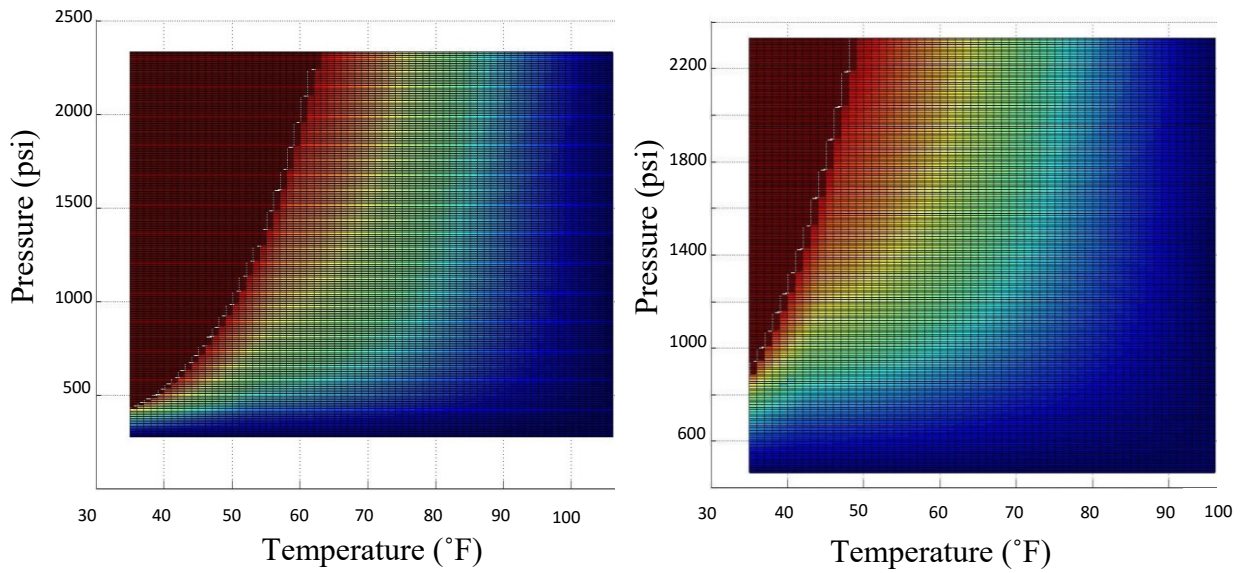


Figure 2-5: (a) Probability values for 99% CH<sub>4</sub> & 1% C<sub>2</sub>H<sub>6</sub>, (b) Probability values for 99% CH<sub>4</sub>, 1% C<sub>2</sub>H<sub>6</sub> & MeOH 10 wt%

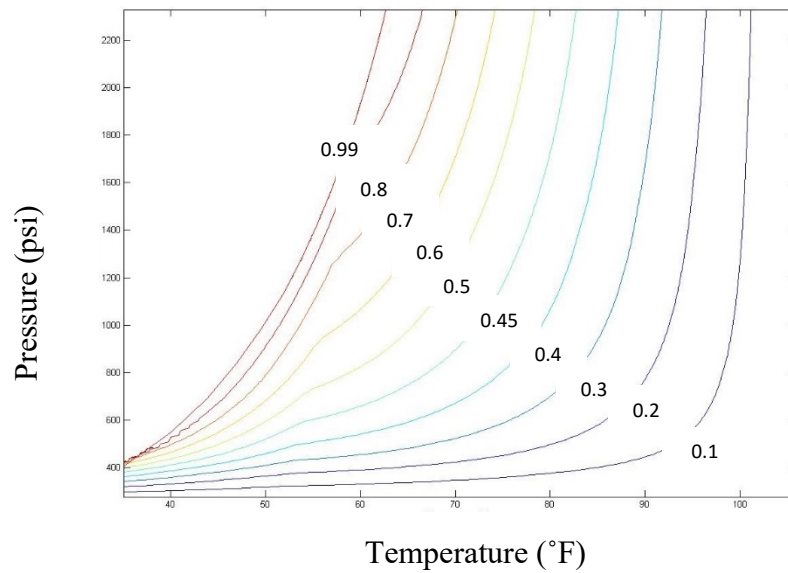


Figure 2-6: Hydrate formation probability curves

### 2.3.2 Case study II

Figure 2-7 presents the pressure-temperature diagram for a deepwater flowline fluid from a case study presented by Notz (1994). This shows a 50 mile seafloor pipeline from a petroleum well in deepwater. From Figure 2-7, it can be seen that at about 9 miles from the subsea wellhead the system enters the hydrate-stable region and continues to be inside the stable region till 45 miles without the presence of inhibitors. Moreover, 20 wt% methanol is required to shift the hydrate formation curve away (left) from flow conditions to prevent hydrate formation as indicated in the case study.

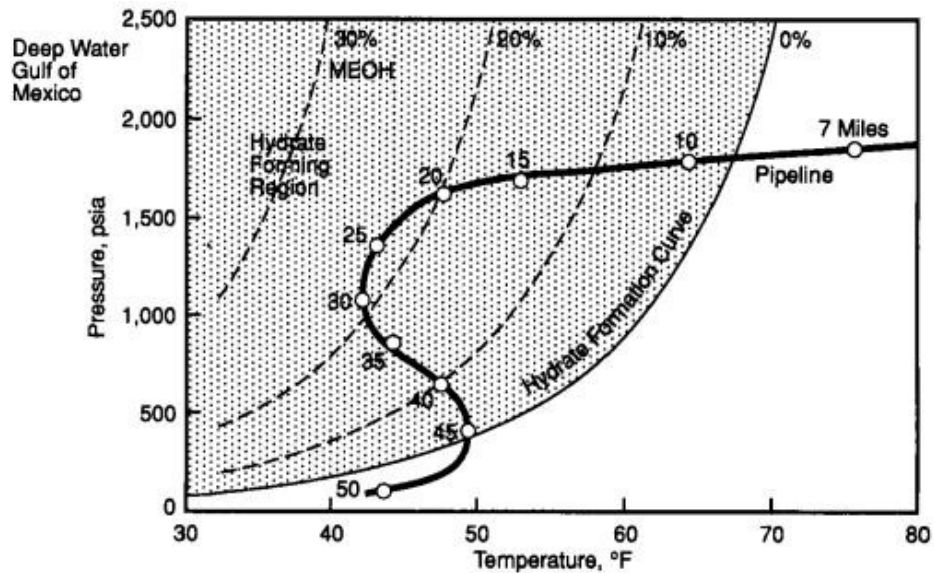


Figure 2-7: Deepwater pipeline with hydrate curves (Notz, 1994)

Probability plots were generated for the two cases: without inhibition and with 20% MeOH as shown in Figure 2-8. For the case without inhibition (Figure 2-8(a)), at 7 miles from the wellhead the probability of hydrate formation is 0.55. For MeOH 20 wt% (Figure 2-8(b)),

the probability of hydrate formation with the same operating conditions decreases to 0.33. Also the gradual increase of hydrate formation probability along the pipe length could be observed (at 10 miles: 0.56, at 15 miles: 0.77)

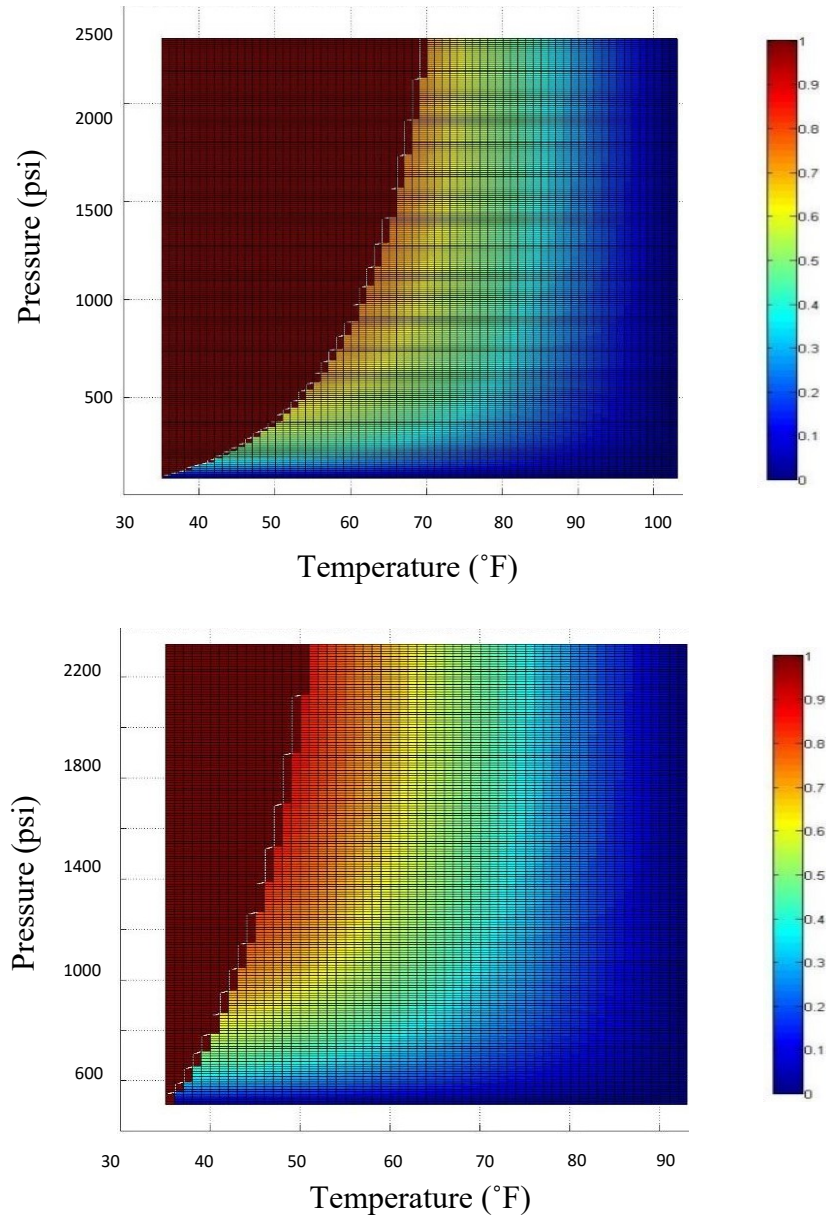


Figure 2-8: (a) Probability values without inhibition, (b) Probability values with MeOH 20 wt%

## 2.4 Validation of the proposed method

Due to the lack of data available for transient temperature and pressure conditions of oil and gas production/transportation pipelines, the validation of the proposed method is carried out in an alternate approach. As shown in Figure 2-7 (Case study II), the use of inhibitors will shift the hydrate formation curve towards lower temperatures. For validation of the proposed method, we considered the shift of the hydrate formation curve for a given composition and concentration of inhibitor in weight percent in the aqueous phase. Then probability curves were generated for two cases: with and without inhibitors to establish a firm relationship and/or pattern within the curves of similar probability values. The temperature depression due to inhibition was calculated and compared with the average temperature difference between the probability curves. It provides a solid relationship between the probability curves developed, which are unique and inherent to the equilibrium curves of the respective compositions. Hence, this validates the accuracy of the proposed method. This is achieved by comparing the mean difference between curves with the same probability values of different compositions. In this case, the compositions of 99% methane and 1% ethane without inhibitors and with MeOH 10 wt% are considered.

As shown in Figure 2-9, for the two cases considered (with and without inhibitors), the average difference between probability curves is calculated for 10 sets of curves with probabilities ranging from 0-1 and tabulated (Table 2-1) to compare the deviation of each average difference with the mean.

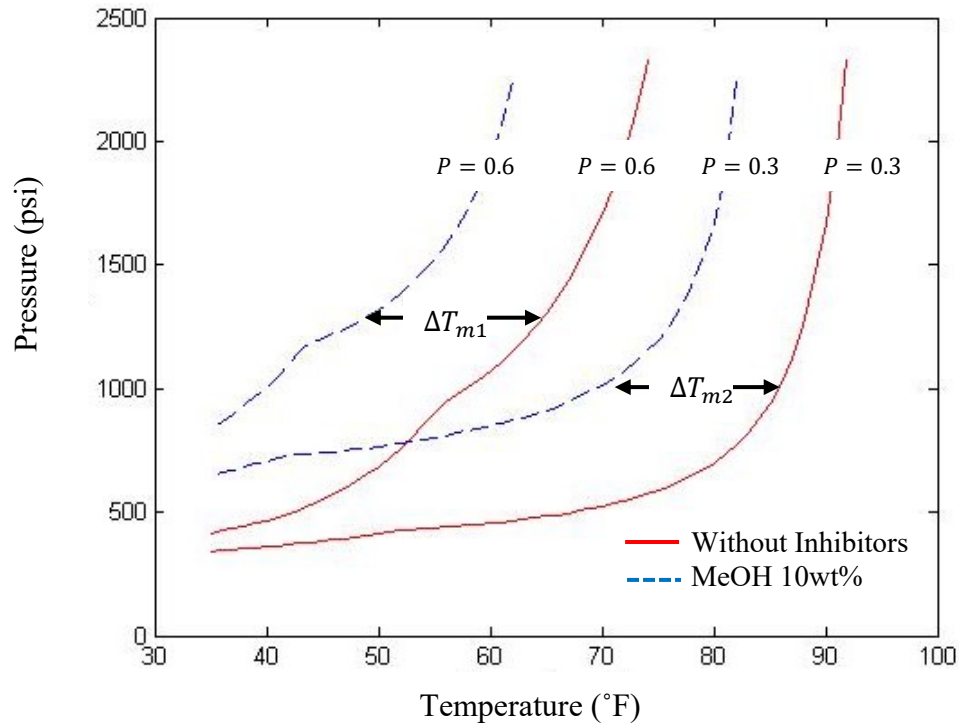


Figure 2-9: Average difference between probability curves

Nielsen and Bucklin (1983) proposed an equation (Eq. 2-5) to calculate the temperature depression of the hydrate curve due to inhibition and suggested it could be effectively used for methanol injection systems.

$$\Delta T = -129.6 \ln(1 - x_{MeOH}) \quad (2-5)$$

where  $\Delta T$  is the temperature depression due to inhibition ( $^{\circ}\text{F}$ ) and  $x_{MeOH}$  is the mole fraction of inhibitor in liquid phase. Although Nielsen-Bucklin equation was developed to use with methanol, the equation is independent of the type of inhibitor and is claimed to be accurate up to 90 wt% methanol (Mokhatab, Poe, & Mak, 2015). A recent study

(Moshfeghian, 2007) evaluated the accuracy of three methods (Hammerschmidt, Nielsen-Bucklin and Moshfeghian-Maddox) developed to calculate the temperature depression in the presence of inhibitors and concluded that Moshfeghian-Maddox method gives better results than Nielsen-Bucklin method for lower temperatures.

Table 2-1: Percentage deviation of average difference from the mean

<b>Probability of hydrate formation</b>	<b>Average difference <math>\Delta T_{mi}</math></b>	<b>Deviation from mean %</b>
0.1	13.045	7.28
0.2	14.005	0.46
0.3	14.643	4.07
0.4	14.723	4.64
0.45	14.649	4.11
0.5	14.586	3.66
0.6	14.18	0.78
0.7	13.80	1.91
0.8	13.575	3.52
0.9	13.492	4.11

Using Eq.5, for a system with 10 wt% methanol injection, the temperature shift of the hydrate curve can be calculated as 13.66°F. From the results obtained (Table 2-1), the average temperature difference between the probability curves i.e., temperature depression due to inhibition, is 14.06°F. Therefore, the probability curves satisfy the temperature shift due to inhibition with a very small error (~2.9%). Moreover, from Table 2-1, it can be seen that the maximum percentage deviation of the average temperature difference ( $\Delta T_{mi}$ ) with respect to its mean value is 7.28% (for probability values ranging from 0.1-0.9). Therefore, from the results obtained it is evident that, irrespective of the compositions considered, the probability curves generated from the proposed method are correlated to the respective hydrate equilibrium curves in a similar manner with a percentage deviation of less than 8%. This in turns demonstrates the accuracy and robustness of the proposed calculation method, since the probability curves strictly follow a pattern which is correlated to the respective hydrate equilibrium curves.

## 2.5 Conclusions

A novel methodology is developed to predict the probability of hydrate formation in subsea pipelines for any given composition and operating condition (temperature and pressure). The proposed method considers all possible pathways in reaching hydrate forming conditions, though for a real life scenario it may not necessarily be true at all times. Therefore, depending on the process conditions of the considered system, the achievable pathways can be changed accordingly. The proposed method is validated by comparing the

probability curves of different compositions, thus obtaining a strong relationship between the curves irrespective of the compositions.

Due to the simplicity of the proposed methodology, it can be easily adopted to any oil and gas pipeline with known composition and operating conditions to predict the probability of hydrate formation without the hassle of prolonged gathering of data. Moreover, this method can be effectively used to quantify the effect of inhibition in terms of probability and can be considered as the initial phase towards hydrate risk assessment exercise.

The focus of the present study is limited to the right hand side of the hydrate forming curve to determine the probability of hydrate formation where the hydrate forming curve is assigned a probability of 1 for the ease of model development. It is important to note that, hydrates do not necessarily form even if the operating conditions reach the temperature and pressure conditions of the hydrate equilibrium curve, since a certain amount of subcooling and induction time is required for hydrates to transfer into the stable region. Therefore, in future work, the effect of subcooling and induction time can be taken into consideration to expand the proposed method towards the metastable region of hydrates. Furthermore, the temperature drop due to heat losses and pressure drop due to frictional losses can be associated with the proposed model by assigning weightage to the most-likely temperature-pressure profile along the pipeline to minimize limitations. The proposed approach can be further advanced by integrating updating mechanisms (ex: Bayesian) to achieve better approximations for the probability of hydrate formation. Further, the proposed method can be adapted in risk based hydrate prevention schemes, i.e., inhibition and heat tracing requirements.

## 2.6 References

- Bai, Y., & Bai, Q. (2012). *Subsea Engineering Handbook*. Gulf Professional Publishing.
- Carroll, J. (2009). *Natural Gas Hydrates: A Guide for Engineers*. Gulf Professional Publishing.
- Carson, D. B., & Katz, D. L. (1942). Natural Gas Hydrates. *Transactions of the AIME*, 146, 150.
- Davies, S. R., Boxall, J., Koh, C. A., Sloan, E. D., Hemmingsen, P., Kinnari, K. J., & Xu, Z.-G. (2008). Predicting Hydrate Plug Formation in a Subsea Tieback. Society of Petroleum Engineers. <http://doi.org/10.2118/115763-MS>
- Deng, D., Tu, D., Dong, Y., Geng, L., & Gong, J. (2014). Calculation of hydrate formation probability in wet-gas pipelines. *CIESC Journal*, 65(6), 2270–2275. <http://doi.org/10.3969/j.issn.0438-1157.2014.06.043>
- Elgibaly, A. A., & Elkamel, A. M. (1998). A new correlation for predicting hydrate formation conditions for various gas mixtures and inhibitors. *Fluid Phase Equilibria*, 152(1), 23–42. [http://doi.org/10.1016/S0378-3812\(98\)00368-9](http://doi.org/10.1016/S0378-3812(98)00368-9)
- Kashchiev, D. (2000). *Nucleation*. Butterworth-Heinemann.
- Kashchiev, D., & Firoozabadi, A. (2003). Induction time in crystallization of gas hydrates. *Journal of Crystal Growth*, 250(3–4), 499–515. [http://doi.org/10.1016/S0022-0248\(02\)02461-2](http://doi.org/10.1016/S0022-0248(02)02461-2)
- Lederhos, J. P., Long, J. P., Sum, A., Christiansen, R. L., & Sloan Jr, E. D. (1996). Effective kinetic inhibitors for natural gas hydrates. *Chemical Engineering Science*, 51(8), 1221–1229. [http://doi.org/10.1016/0009-2509\(95\)00370-3](http://doi.org/10.1016/0009-2509(95)00370-3)

- Mokhatab, S., Poe, W. A., & Mak, J. Y. (2015). *Handbook of Natural Gas Transmission and Processing: Principles and Practices*. Elsevier Science Limited.
- Mokhatab, S., & Towler, B. (2005). Quickly estimate hydrate formation conditions in natural gases. *Hydrocarbon Processing*, 61–2.
- Moshfeghian, M. (2007, January 8). Study tests accuracy of methods that estimate hydrate formation. *Oil & Gas Journal*, p. 44. John M. Campbell & Co. Norman, Okla.
- Motiee, M. (1991). Estimate Possibility of Hydrates. *Hydrocarbon Processing*, 70(7), 98–99.
- Nielsen, R. B., & Bucklin, R. W. (1983). Why Not Use Methanol for Hydrate Control? *Hydrocarbon Processing*, 62(4), 71.
- Notz, P. K. (1994). Discussion of the Paper “The Study of Separation of Nitrogen from Methane by Hydrate Formation Using a Novel Apparatus.” *Annals of the New York Academy of Sciences*, 715(1), 425–429. <http://doi.org/10.1111/j.1749-6632.1994.tb38855.x>
- Seo, Y., & Kang, S.-P. (2012). Inhibition of methane hydrate re-formation in offshore pipelines with a kinetic hydrate inhibitor. *Journal of Petroleum Science and Engineering*, 88–89, 61–66. <http://doi.org/10.1016/j.petrol.2011.11.001>
- Sloan, E. D. (1998). *Clathrate Hydrates of Natural Gases, Second Edition, Revised and Expanded*. CRC Press.
- Sloan, E. D. (2003). Fundamental principles and applications of natural gas hydrates. *Nature*, 426(6964), 353–363. <http://doi.org/10.1038/nature02135>

- Sloan, E. D. (2005). A changing hydrate paradigm—from apprehension to avoidance to risk management. *Fluid Phase Equilibria*, 228–229, 67–74.  
<http://doi.org/10.1016/j.fluid.2004.08.009>
- Urdahl, O., Børnes, A. H., Kinnari, K. J., & Holme, R. (2004). Operational Experience by Applying Direct Electrical Heating for Hydrate Prevention. *SPE Production & Facilities*, 19(03), 161–167. <http://doi.org/10.2118/85015-PA>
- Wu, M., Wang, S., & Liu, H. (2007). A Study on Inhibitors for the Prevention of Hydrate Formation in Gas Transmission Pipeline. *Journal of Natural Gas Chemistry*, 16(1), 81–85. [http://doi.org/10.1016/S1003-9953\(07\)60031-0](http://doi.org/10.1016/S1003-9953(07)60031-0)
- Wu, R., Kozielski, K. A., Hartley, P. G., May, E. F., Boxall, J., & Maeda, N. (2013). Probability distributions of gas hydrate formation. *AIChE Journal*, 59(7), 2640–2646. <http://doi.org/10.1002/aic.14037>
- Zerpa, L. E., Sloan, E. D., Sum, A. K., & Koh, C. A. (2012). Overview of CSMHyK: A transient hydrate formation model. *Journal of Petroleum Science and Engineering*, 98–99, 122–129. <http://doi.org/10.1016/j.petrol.2012.08.017>

## **Chapter 3. Risk-based Winterization to Prevent Hydrate Formation in Northern Harsh Environment**

Dinesh Herath, Faisal Khan, Ming Yang

*Safety and Risk Engineering Group (SREG), Faculty of Engineering and Applied Science, Memorial University of Newfoundland, St. John's, NL, Canada*

### **Abstract**

With the increasing demand for energy around the globe, hydrocarbon explorations move towards the Arctic region that holds a majority of unexploited oil reserves. The harsh environmental conditions with sub-zero ambient temperatures and high winds demand winterization techniques for pipes, instruments and equipment to carry out uninterrupted plant operations. The natural phenomenon: hydrate formation, is considered to be a major flow assurance problem starting from the wellhead through the final point in the delivery system which could be addressed through winterization. Developing winterization strategies for arctic conditions is a challenging task demanding rigorous and robust approaches. Risk-based winterization is a novel approach, adapted for vessels operating in arctic environments. In this paper a new model is proposed to calculate the probability of hydrate formation and its associated risk for a given loading scenario. The winterization requirement is determined based on the estimated risk. Two case studies presented here demonstrate the applicability of the proposed model and compare several winterization methods to find an optimal solution.

Keywords: Winterization, Hydrate formation, Natural gas pipeline, Heat transfer, Risk assessment

### **3.1 Introduction**

Oil and gas exploration move towards the Arctic region with the ever-rising demand for energy. More than 25% of the world's unexploited oil reserves are held by the Arctic offshore ("The challenges facing arctic pipelines," n.d.). However, the extreme weather conditions in the Arctic region pose many difficulties for operational and development activities. Since most of the guidelines and regulations are specified in a more general form addressing both onshore and offshore applications, new modified industry guidelines and regulations are required for more reliable use in Arctic conditions. DNV offshore standards specify general principles for the preparation of mobile units and offshore installations in cold-climate conditions.

In Arctic conditions, design and operations are faced with many challenges such as winterization, flow assurance, permafrost thaw, ice gouging and upheaval buckling. Most of the aforementioned challenges do not apply elsewhere other than the Arctic region. In harsh Arctic environments where ambient temperatures are below freezing with high winds, winterization methods are necessary in the oil and gas industry for pipes, instruments and equipment to carry out uninterrupted plant operations. When providing solutions for any challenges faced in harsh environments, both safety and economic aspects should be taken into consideration. The decision making process of winterization is

generally based on engineering judgment and experience where multiple factors as shown in Figure 3-1 play a major role.

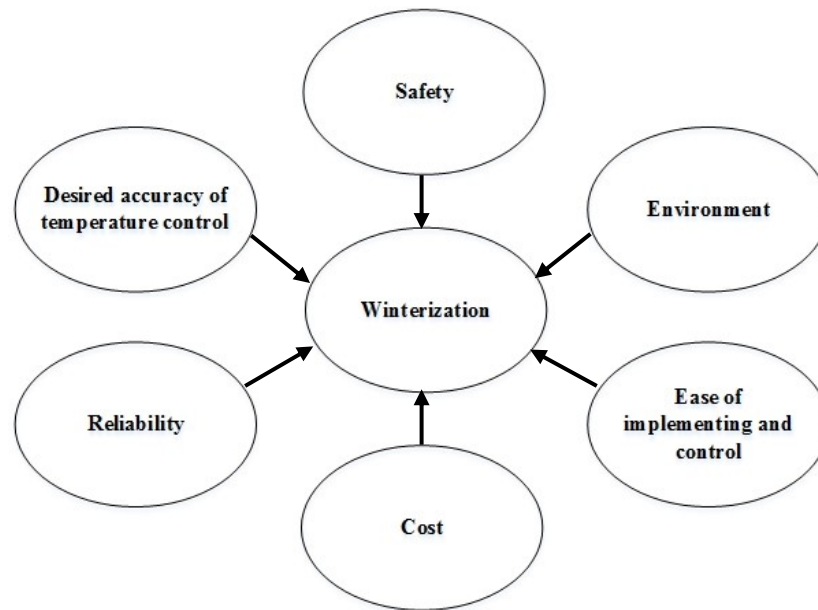


Figure 3-1: Factors affecting the decision making process of winterization

Designing a system/component for a specific winterization level based solely on traditional methods such as theoretical calculations may lead to over-winterization, which increases cost. This is expected since the minimum temperature is observed at low frequencies. Risk-based winterization is a novel approach which supports “evaluation and selection of winterization technologies” based on a “risk-based decision support framework”. Yang et al. adapted a risk-based winterization technique for vessels operating in Arctic environments (Yang & Khan, 2013). Application of winterization methods for vessels

operating in Arctic conditions is an active research area (Brazil, Conachey, Savage, & Baen, 2013),(Baen & Oldford, 2014), and many organizations have provided guidelines for hull construction: American Bureau of Shipping (ABS), Norwegian Classification Society (DNV), Russian Classification Society (RMRS) and International Organization for Standardization (ISO) 19906.

The natural phenomenon: freezing, is a common occurrence in natural gas pipeline systems and poses a potential threat to continuous production as well as to the safety and integrity of the facility. Similarly, hydrate formation is considered to be a serious problem starting from the wellhead through the final point in a delivery system. Though hydrate formation is different from ice formation (freezing), it could be addressed in a similar manner in terms of winterization. When determining the extent of winterization for a natural gas pipeline, factors such as ambient temperature, operating conditions, rate of snowfall and wind velocity need to be taken into consideration.

It is important to note that both internal and external involvements play a similar role in hydrate formation. The majority of studies carried out are related to internal involvement, where change of operating conditions (e.g. temperature, pressure, water-cut), mechanisms of hydrate formation (e.g. shell growth model), effect of flow parameters (e.g. viscosity, density, velocity) and geometric parameters (e.g. pipe diameter) are the key focus areas. Although both temperature and pressure conditions must be satisfied for hydrate formation, temperature plays the dominant role, due to extreme cold weather conditions in the Arctic environments. This study mainly focuses on the external factors (e.g. extreme low

temperature) and its effect on hydrate formation in pipelines operating in harsh environments.

### **3.2 Hydrate Formation**

Hydrate formation is considered as one of the major flow assurance problems faced in the oil and gas industry which may result in blockage of pipelines and equipment (Sloan, 1998). Pipelines carrying natural gas are more susceptible to bursting and explosion as a result of hydrate plugging. Furthermore, formation of hydrates can alter flow measurements or block instrumentation supply lines that will hamper control of the systems.

With increasing deepwater operations and Arctic explorations, hydrate formation has become a prime issue in the oil and gas industry. Up to 8% of the total estimated operating cost spent by the oil and gas industry is to restrain hydrate formation while hydrate inhibition costs are estimated at 220 million dollars annually (Sloan, 2003). Hydrates, often referred to as clathrate hydrates, may form at any location in a production/processing system which has natural gas and water with favorable operating conditions (i.e., high pressure and low temperature as shown in Figure 3-2).

Hydrate forming curves are used to define the pressure and temperature conditions at which hydrates tend to form. Figure 3-2 shows a typical hydrate forming curve with a pressure-temperature diagram for a deepwater flowline fluid from a case study presented by Notz (1994). Operating conditions to the left side of the hydrate formation curve fall into the hydrate-stable region while the right side of the curve is a hydrate-free region. From Figure

3-2, it can be seen that at about 9 miles from the subsea wellhead the system enters the hydrate-stable region and continues to be in the stable region till 45 miles without the presence of inhibitors. Figure 3-2 also presents the effect of inhibition, a commonly used winterization scheme. It can be clearly seen that with increasing inhibitor percentages the hydrate forming curve shifts toward lower temperatures, where 23 wt% methanol is required to shift the hydrate formation curve away (left) from operating flow conditions to prevent hydrate formation, as indicated in the case study. Likewise, winterization requirements are often based on approximate theoretical values and laboratory tests (Brazil, Conachey, Savage, & Baen, 2012) which provide more conservative values. Therefore, in present work, a rigorous risk-based approach is proposed to assess winterization requirements.

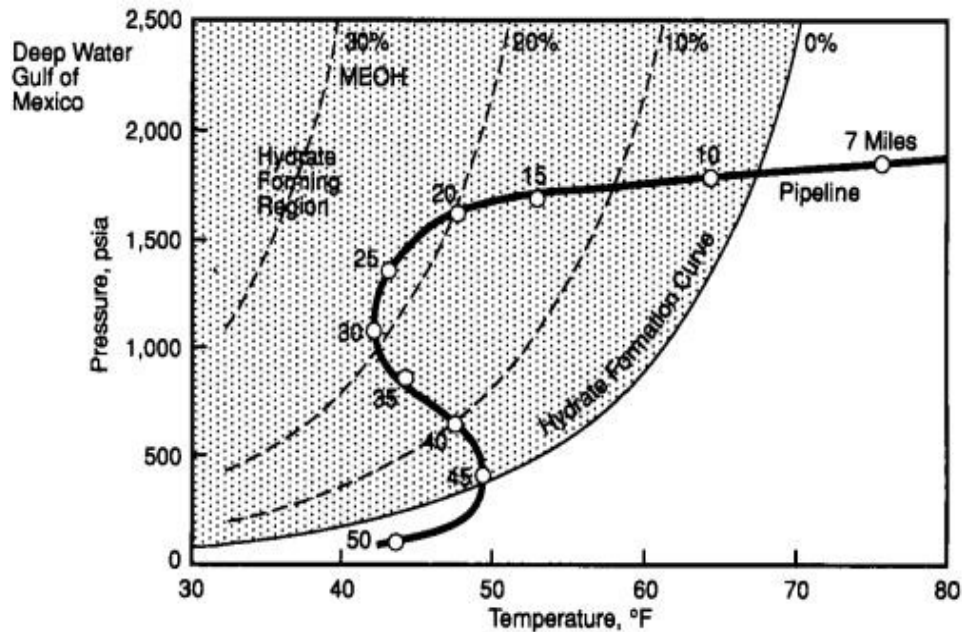


Figure 3-2: Deepwater pipeline with hydrate curves [Notz, 1994]

Different methods/approaches have been developed to predict hydrate forming pressure and temperature, of which the K-factor (Carson & Katz, 1942) method is most frequently referred to in the literature. Several other correlations based on the gas gravity method to ascertain hydrate forming conditions are found in literature, such as in the work of Elgibaly and Elkamel (Elgibaly & Elkamel, 1998), Towler and Mokhatab (Mokhatab & Towler, 2005), Motiee (Motiee, 1991). With the advancement of computer technology, tools dedicated to hydrate calculations such as CSMHYD (Sloan, 1998) have been developed, replacing approximate hand calculation methods. Nowadays, most of the commercially available process simulation software (e.g., PVTsim, PIPESIM, Hysys) is capable of predicting hydrate forming conditions.

### **3.3 Risk-based Winterization Approach to Prevent Hydrate Formation**

The major steps of the proposed risk-based winterization methodology to prevent hydrate formation are presented in Figure 3-3. Each of the major steps is described in detail in the following sections, with illustrative examples.

#### **3.3.1 Identify the criticality of the system**

As the initial step, criticality of the selected pipeline is determined. A quantification scheme for the severity levels of consequences is carried out based on the criticality of the considered system where severity values are assigned to each consequence based on several factors such as: injuries/fatalities, environmental damage, financial losses or loss of productivity. A risk matrix is shown in Figure 3-4 with four risk levels: very high, high,

medium and low, as the product of the Probability of Hydrate Formation (PoHF) and severity value. The acceptable risk level for a specific system is defined according to operators' requirements and the risk matrix is customized accordingly.

Once the criticality of the system is determined, the likelihood of hydrate formation is calculated as illustrated in the following sections. The current work is focused on reducing the likelihood of hydrate formation which in turn will reduce the associated risk to an acceptable level.

### **3.3.2 Environmental load**

Prior to risk-based analysis presented in the following sections, environment load is estimated for the region considered. Environmental load can be expressed as a function of two variables: ambient temperature and its duration. For the probabilistic estimations of hydrate formation, it is required to express temperature in probabilistic distributions. For load conditions, this is achieved by gathering hourly temperature data for at least 20 years and calculating average temperatures over defined time intervals to determine the loading temperature in probabilistic terms. Sulistryono et. al proposed a novel methodology to assess environmental load using a statistical approach based on magnitude and frequency, which is adaptable for risk-based winterization strategies (Sulistryono et al., 2014).

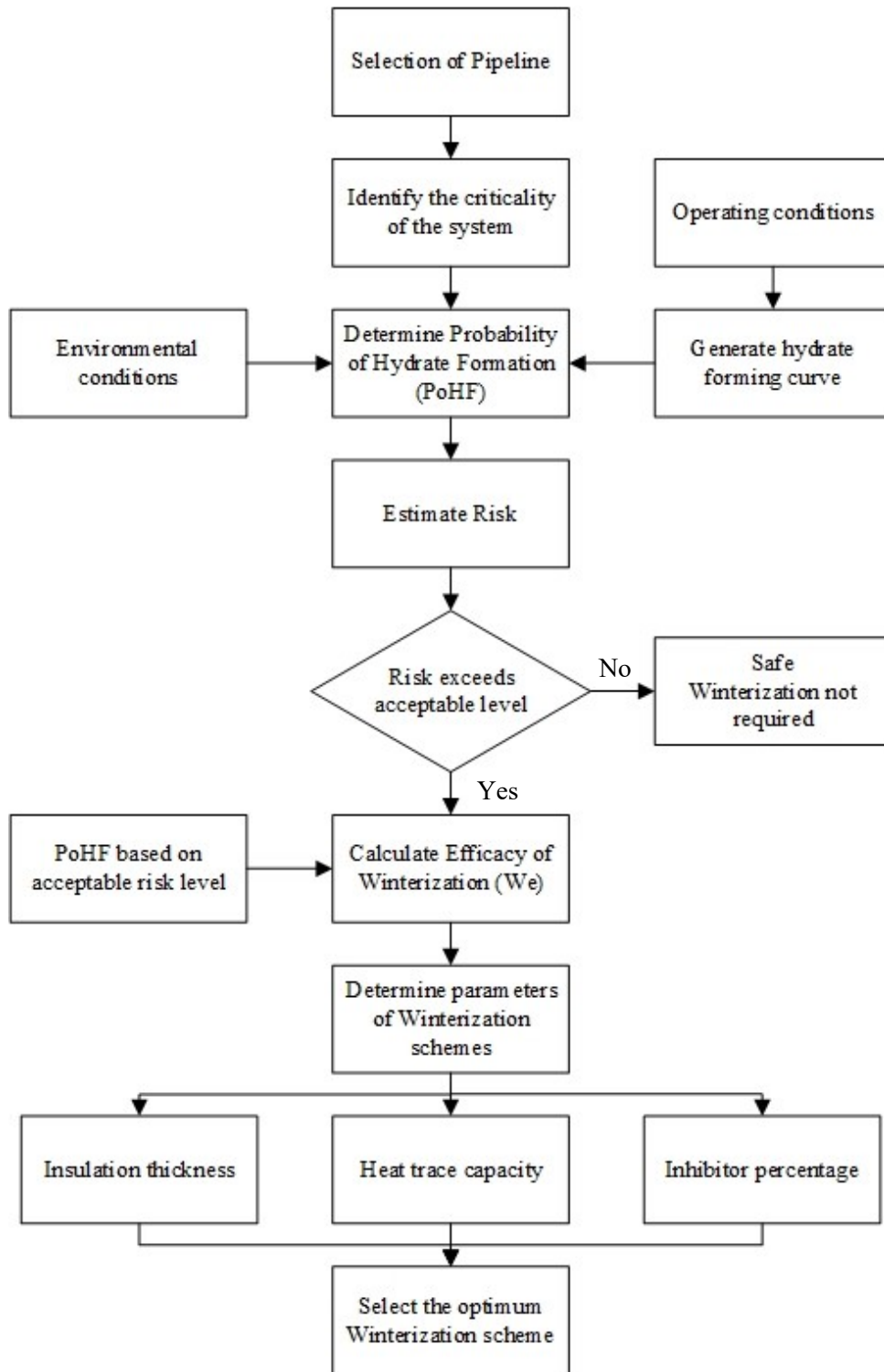


Figure 3-3: Risk-based winterization approach to prevent hydrate formation

		<b>Consequences</b>				
		Negligible (0-2)	Minor (2-4)	Moderate (4-6)	Critical (6-8)	Catastrophic (8-10)
Probability	Very Likely (1-0.1)	Medium	High	High	Very High	Very High
	Likely (0.01-0.1)	Medium	Medium	High	Very High	Very High
	Possible (0.001-0.01)	Low	Medium	Medium	High	Very High
	Unlikely (0.0001-0.001)	Low	Low	Medium	High	High
	Very Unlikely (<0.0001)	Low	Low	Low	Medium	High

Figure 3-4: Risk matrix

### 3.3.3 Estimation of Probability of Hydrate Formation (PoHF)

A limit state function (Eq. 3-1) is developed to calculate the probability of hydrate formation.

$$g(x) = |\Delta T_{system}| - |\Delta T_{min}| \quad (3-1)$$

$$|\Delta T_{system}| = |L - T_{op}| \quad (3-2)$$

where  $|\Delta T_{system}|$  is the difference between the load and the operating envelop ( $T_{op}$ ).  $|\Delta T_{min}|$  is defined as the minimum allowable temperature difference between the load and the operating temperature to maintain the system in the hydrate free region. Several factors need to be considered when defining  $|\Delta T_{min}|$  such as the operating conditions (temperature and pressure), gas composition and load temperature.  $|\Delta T_{min}|$  is obtained following the steps shown in Figure 3-5.

If the actual temperature difference of the system is less than the specified minimum temperature difference, the system will fall into the hydrate-stable region. Therefore, it is considered that if the actual temperature difference of the system falls below the minimum temperature difference ( $|\Delta T_{sys}| < |\Delta T_{min}|$ ) there will be a fail state (Hydrates formed). i.e.  $g(x) < 0$ . Hence, the probability of hydrate formation (PoHF) can be expressed as:

$$\text{PoHF} = \Pr(|\Delta T_{sys}| < |\Delta T_{min}|) = \int_{-\infty}^{|\Delta T_{min}|} f_{\Delta T_{sys}}(\Delta T_{sys}) d\Delta T_{sys} \quad (3-3)$$

Where,  $f_{\Delta T_{sys}}$  is the probability density function of  $|\Delta T_{sys}|$ .

For a constant pressure system, the limit state function simplifies to:

$$g(x) = T_{op} - T_{eq} \quad (3-4)$$

where  $T_{eq}$  is the hydrate equilibrium temperature corresponding to the given operating conditions. Therefore, for a system with specific gas composition and temperature distribution with known parameters, simulation methods such as the Monte Carlo method could be adapted to determine the probability of hydrate formation.

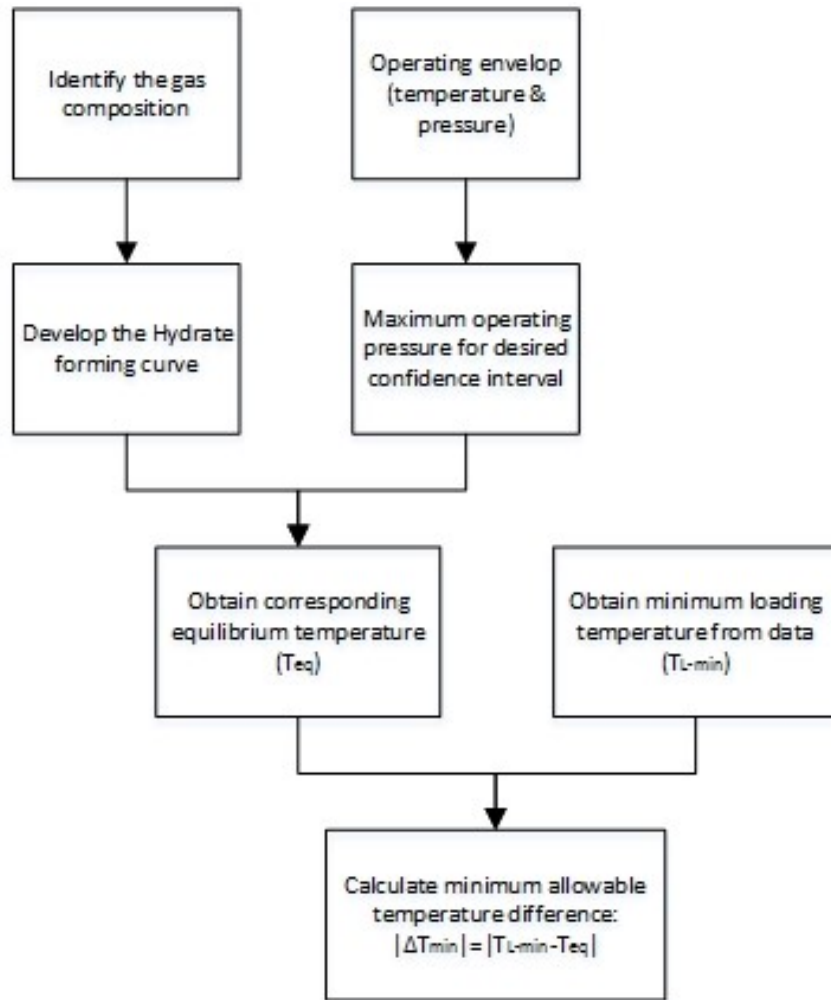


Figure 3-5: Method to obtain the minimum allowable temperature difference

For the purpose of illustration, consider a natural gas pipeline system in Arctic conditions which needs to be winterized with the following characteristics of fluid and environmental conditions:

- (i) Gas composition: 99% CH<sub>4</sub>, 1% C<sub>2</sub>H<sub>4</sub>

- (ii) Load: follows normal distribution with average temperature  $\mu_L = -28.5^\circ\text{C}$  and standard deviation  $\sigma_L = 1.2^\circ\text{C}$
- (iii) Operating conditions: temperature follows normal distribution with  $\mu_{T,op} = 12.5^\circ\text{C}$  and  $\sigma_{T,op} = 1.5^\circ\text{C}$ , pressure follows normal distribution with  $\mu_{P,op} = 1025$  psi and  $\sigma_{P,op} = 60$ psi

As the first step, a hydrate forming curve is developed for the considered gas composition using PVTsim. As shown in Figure 3-6, the minimum observed load temperature and equilibrium temperature corresponding to the maximum pressure of the operating envelope are to be considered when obtaining the minimum allowable temperature difference. A desired level of confidence is to be considered to calculate the minimum load temperature and maximum operating pressure from the respective distributions.

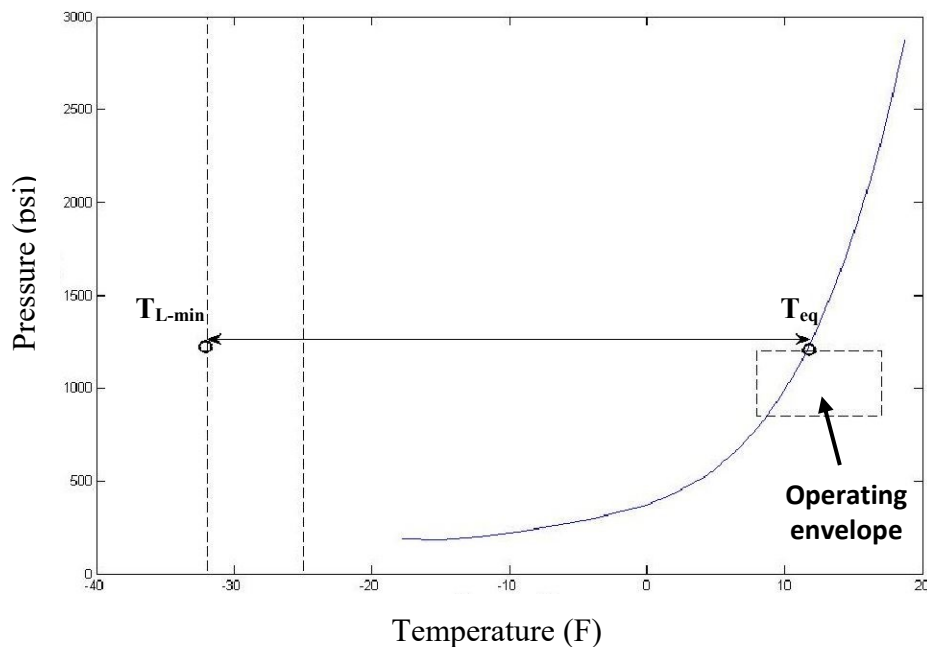


Figure 3-6: Hydrate formation curve- Minimum allowable temperature

For a 99% confidence interval  $T_{L-min} = -32^{\circ}\text{C}$  and  $P_{OP-max} = 1200$  psi. Therefore as shown in Figure 3-6, the corresponding equilibrium temperature,  $T_{eq} = 12^{\circ}\text{C}$ . Since  $|\Delta T_{min}| = |T_{L-min} - T_{eq}|$ , the minimum allowable temperature is calculated as  $44^{\circ}\text{C}$ .

From Eq. 3-2, as  $|\Delta T_{system}| = |L-T_{OP}|$ , the temperature difference of the system also follows a normal distribution with parameters:  $\mu_{system} = 41^{\circ}\text{C}$  and  $\sigma_{system} = 1.92$

Using Eq.3-3,

$$PoHF = \Phi\left(\frac{|\Delta T_{min}| - \mu}{\sigma}\right) = \Phi\left(\frac{44 - 41}{1.92}\right) = 0.94$$

Therefore the likelihood of hydrate formation in the pipeline with the given conditions is high, with an estimated value for probability of hydrate formation of 0.94.

### 3.3.4 Risk estimation

Risk is simply defined as the product of consequences and probability of failure, following the traditional definition of risk.

$$\text{Risk} = \text{Consequences} \times \text{Probability of failure}$$

Therefore, risk is a function of the likelihood of hydrate formation and its associated consequences. Consequences are the outcomes/results of an event where an initial consequence may lead to a series of consequences due to knock-on effects. Since the current work is focused on reducing the likelihood of hydrate formation, the value of risk for any considered system is solely driven by the probability of hydrate formation.

Using the previous example, for a pipeline with a severity value of 4, the risk can be calculated as:

$$\begin{aligned}\text{Risk} &= 0.94 \times 4 \\ &= 3.76\end{aligned}$$

Therefore, from the risk matrix (Figure 3-4), the risk is considered to be high, which indicates the demand for winterization methods.

### 3.3.5 Winterization methods

To mitigate freezing problems, different solution methods can be applied based on the specific requirements of the considered system. Since each solution method may have advantages as well as disadvantages, it is important to select the optimal winterization method(s) which would permit consistent operation of the system.

#### *a) Insulation*

Insulation is one of the primary and efficient mode of winterization techniques. Insulation slows down the rate of heat loss from a pipe to the environment. However, insulation alone is not sufficient to maintain a pipeline inside hydrate-free zone; therefore it should be used in conjunction with other modes of winterization such as application of heat. Since insulation reduces the rate of heat loss, it will also reduce the amount of heat required for maintaining a specific temperature. Insulation thickness should be calculated as a function of the ambient temperature and the operating conditions of the pipeline.

### *b) Application of Heat*

For a pipeline with known gas composition, hydrate forming conditions can be calculated using any method, as described in Section 3.2. Therefore, one could merely maintain the operating temperature of the pipeline above the hydrate forming temperature to avoid hydrate formation. Heat tracing is the commonly used method of heat application.

Heat tracing is an active winterization technique, since it is capable of supplying the amount of heat necessary for efficient flow (i.e. without hydrate formation/freezing) only when required. Also, it is a reliable method of winterization which is capable of providing uniform and controllable heat to the pipeline. There are two types of heat tracing methods available: electrical or fluid medium, where in both cases the heat trace is in physical contact along the length of the pipeline.

- **Electric Heat Tracing**

Electric heat tracing is the preferred method of heat addition due to its higher accuracy of temperature control than with other methods. Typically, an electric heat tracing system comprises a heating cable (conductor), temperature measurement sensor, a controller panel and a relay. Electric heat tracing systems are preferred over thermal systems mainly due to their accurate temperature control and efficiency. Depending on the application, there are two types of electrical heat trace cables available: constant wattage and self-limiting/self-regulating cable. Constant wattage cables are designed to deliver a certain amount of wattage per linear foot at a particular voltage, while the self-limiting type has the ability to self-regulate its power output in relation to the ambient conditions.

- Thermic Fluid

This method of heat tracing may be considered economical if used for large heat requirements. Unlike electric heat tracing, the fluid medium is limited to applications that demand less accuracy. Also, thermic fluid requires high maintenance due to the inherent safety issues caused by leakages.

Though steam heat tracing is capable of providing high heat output with minimal cost (since steam is produced from processed heat), it is not preferred for offshore facilities mainly due to the added complexity, insufficient availability of fresh water and safety related issues.

Heat tracing can be used in conjunction with heat conservation methods such as insulation for improved efficiency. Though freeze protection (winterization) is the main purpose of heat tracing, it is also applicable to maintain viscosity and prevent condensation. Appropriate safety measures must be addressed when using a heat source since it can be a potential hazard by providing an ignition source for hydrocarbons.

### *c) Inhibition*

Alcohols, glycols and ionic solids are common thermodynamic inhibitors. The addition of inhibitors shifts the hydrate equilibrium curve towards lower temperatures which reduces the temperature or increases the pressure at which hydrates form. Methanol is the most popular of alcohols due to its low cost and effectiveness, whereas ethylene glycol (EG or MEG) and tri-ethylene glycol are the preferred glycols in the natural gas industry. Inhibitors are injected into the gas stream either using chemical injection pumps or drips.

The temperature depression due to inhibition can be calculated by the formula suggested by Hammerschmidt (1934):

$$\Delta T = \frac{K_H W}{M(100 - W)} \quad (3-5)$$

where,

$\Delta T$ : Temperature depression °C

$K_H$ : Constant (for MeOH: 1297)

$W$ : Concentration of the inhibitor in weight percent in the aqueous phase

$M$ : Molar mass of inhibitor g/mol

The Hammerschmidt formula (Eq. 3-5) is still widely being used in the natural gas industry to approximate the temperature depression due to inhibition, as a primary check (Sloan, Jr & Koh, 2007). Later, Nielsen and Bucklin (Nielsen & Bucklin, 1983) proposed a modified version of the Hammerschmidt equation which could be effectively used for methanol injection systems.

$$\Delta T = -129.6 \ln(1 - x_{MeOH}) \quad (3-6)$$

Using these formulae, the desired amount of inhibitor concentration can be calculated.

### 3.3.6 Estimation of Efficacy of Winterization

The limit state function to calculate PoHF after winterization is obtained by introducing a new term: winterization efficacy ( $W_e$ ), to Eq.3-3 as follows:

$$g'(x) = |\Delta T_{sys}| + W_e - |\Delta T_{min}| \quad (3-7)$$

Winterization efficacy ( $W_e$ ) is defined as the ability to prevent hydrate formation of a considered method, which can either be represented probabilistically or by a constant. Similar to section 3.3.3,  $|\Delta T_{sys}| + W_e < |\Delta T_{min}|$  or  $g'(x) < 0$  is considered a failure state. Therefore, PoHF after winterization is calculated by the following equation:

$$\text{PoHF} = \Pr(|\Delta T_{sys}| + W_e < |\Delta T_{min}|) = \int_{-\infty}^{|\Delta T_{min}|} f_{\Delta T'_{sys}}(\Delta T'_{sys}) d\Delta T'_{sys} \quad (3-8)$$

where  $\Delta T'_{sys} = \Delta T_{sys} + W_e$

If  $W_e$  is a constant value, the following equation can be used.

$$\text{PoHF} = \Pr(|\Delta T_{sys}| < |\Delta T_{min}| - W_e) = \int_{-\infty}^{|\Delta T_{min}| - W_e} f_{\Delta T_{sys}}(\Delta T_{sys}) d\Delta T_{sys} \quad (3-9)$$

In Eq. 3-8 and 3-9 both  $|\Delta T_{sys}|$  and  $|\Delta T_{min}|$  are defined similarly as in Eq.3-1.

Following the previous example in Section 3.3.3, assume a pipeline operating under the same conditions needs to be winterized to an acceptable risk level. Considering the acceptable risk level as low and with a severity value of 4, from the risk matrix (Figure 3-4) the maximum acceptable PoHF is 0.001. Using Eq.3-9;

$$PoHF = \int_{-\infty}^{|\Delta T_{min}| - W_e} f_{\Delta T_{sys}}(\Delta T_{sys}) d\Delta T_{sys} = \Phi\left(\frac{(\Delta T_{min} - W_e) - \mu}{\sigma}\right)$$

Since PoHF,  $\Delta T_{min}$ ,  $\mu$  and  $\sigma$  are known parameters,  $W_e$  could be calculated as:

$$0.001 = \Phi\left(\frac{(44 - W_e) - 41}{1.92}\right)$$

$$W_e = 8.933 \text{ } ^\circ\text{C}$$

Therefore, a winterization method with an efficacy of 8.933°C is required. Once  $W_e$  is determined for a desired value of PoHF (section 3.3), parameters of the available winterization schemes (insulation thickness, heat trace capacity and inhibitor percentage) can be determined, which satisfies the efficacy requirement. Since  $W_e$  is expressed in terms of temperature difference, it can be associated with heat transfer equations to determine the required winterization parameters.

### 3.4 Determine the parameters of winterization schemes

The following sections explain the physics behind heat loss from horizontal pipeline and the procedures to follow in determining parameters of winterization schemes using  $W_e$ .

### 3.4.1 Physics behind heat loss from natural gas pipelines

To develop winterization strategies for natural gas pipelines (for both above and below ground configurations) it is of top most importance to have a clear idea of heat transfer rate accounting for both internal and external flows.

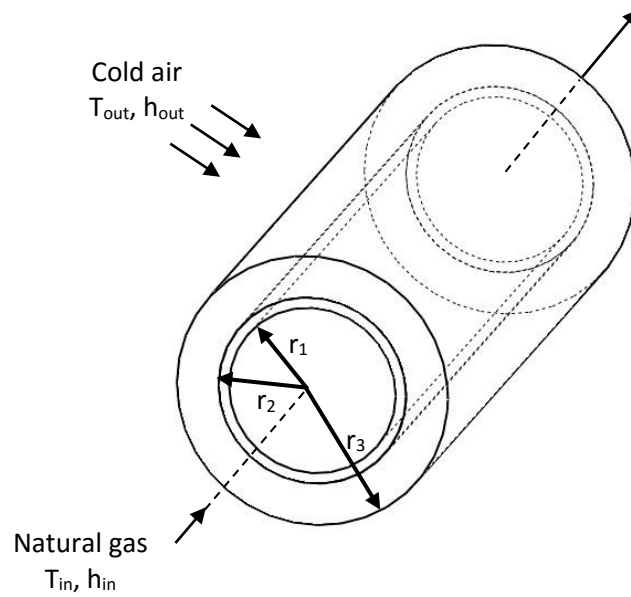


Figure 3-7: Pipe configuration

Considering the heat transfer rate of a cylinder with radial conduction and adapting Fourier's law for a composite system with a pipe thickness:  $r_2-r_1$  and insulation thickness:  $r_3-r_2$  (Figure 3-7), the following equation is obtained (Lienhard IV & Lienhard V, 2003):

$$q = \frac{T_{out} - T_{in}}{\frac{1}{2\pi r_1 L h_{in}} + \frac{\ln r_2/r_1}{2\pi k_A L} + \frac{\ln r_3/r_2}{2\pi k_B L} + \frac{1}{2\pi r_3 L h_{out}}} \quad (3-10)$$

The overall heat transfer coefficient, based on external surface area:

$$U = \frac{1}{\frac{r_3}{r_1 h_{in}} + \frac{r_3 \ln r_2/r_1}{k_A} + \frac{r_3 \ln r_3/r_2}{k_B} + \frac{1}{h_{out}}} \quad (3-11)$$

a.) *External flow*

Many correlations are available to calculate the forced convection heat loss of pipes in cross flow. The correlation proposed by Churchill and Bernstein (Churchill & Bernstein, 1977) is widely used, as it covers the entire range of Reynolds number ( $Re_D$ ) and a wide range of Prandtl number ( $Pr$ ).

$$\overline{Nu}_D = 0.3 + \frac{0.62 Re_D^{1/2} Pr^{1/3}}{[1 + (0.4/Pr)^{2/3}]^{1/4}} \left[ 1 + \left( \frac{Re_D}{282,000} \right)^{5/8} \right]^{4/5} \quad (3-12)$$

where,

$$Pr = \frac{c_p \mu}{k} = \frac{v}{\alpha} \quad (3-13)$$

$$Re = \frac{\rho u D}{\mu} = \frac{u D}{\nu} \quad (3-14)$$

Therefore heat transfer coefficient can be calculated from the following equation:

$$\overline{Nu}_D = \frac{h D}{k} \quad (3-15)$$

All properties are evaluated at the film temperature.

*b.) Internal flow (turbulent)*

For smooth pipes (from Dittus-Boelter equation) (Lienhard IV & Lienhard V, 2003);

$$\overline{Nu}_D = 0.023Re^{0.8}Pr^n \quad (3-16)$$

where, for cooling:  $n = 0.3$ , for heating:  $n = 0.4$ .

Similarly using Eq. 3-15, the heat transfer coefficient for internal flow can be calculated.

All properties are evaluated at the mean bulk fluid temperature.

*c.) Temperature profile along the pipe length*

Steady-flow thermal energy equation:

$$q = \dot{m}C_p\Delta T \quad (3-17)$$

Heat transfer from pipe due to conduction and convection (Newton's law of cooling):

$$q = UA(T_b - T_{out}) \quad (3-18)$$

For an infinitesimal pipe element of length  $dx$  at a position  $x$ , using the above two equations;

$$-\dot{m}C_p dT = U2\pi R dx (T_b - T_{out})$$

It is common practice to assume  $U$ ,  $C_p$ ,  $\dot{m}$  to be constant. Then integrating the above equations from  $T_b(x = 0) = T_0$  to  $T_b(x = L) = T_L$  ;

$$\int_{T_0}^{T_L} \frac{1}{(T_b - T_{out})} dT = - \int_0^L \frac{U2\pi R}{\dot{m}C_p} dx$$

$$T_L = T_{out} + (T_0 - T_{out}) \exp\left(-\frac{U\pi DL}{\dot{m}C_p}\right) \quad (3-19)$$

where U is based on the external surface area,

$$U = \frac{1}{\frac{r_3}{r_1 h_{in}} + \frac{r_3 \ln r_2 / r_1}{k_A} + \frac{r_3 \ln r_3 / r_2}{k_B} + \frac{1}{h_{out}}}$$

From Eq. 3-19, the temperature at any location along the pipeline with a known distance measured from the temperature measuring point can be calculated. Since both  $T_0$  and  $T_{out}$  are distributions, the Monte Carlo simulation methods can be adapted to determine the temperature distribution of the considered location of the pipeline. Then substituting  $T_L$  for  $T_{op}$  in Eq. 3-5, the probability of hydrate formation at any location along the pipeline with a known distance from the temperature measuring point can be obtained.

### 3.4.2 Determination of inhibitor percentage requirement

Following the previous example in section 3.3.3, assume a natural gas pipeline with the same dimensions and gas composition which needs to be winterized using methanol inhibition for an acceptable PoHF value of 0.01. As explained in section 3.3.3, the addition of a hydrate inhibitor will shift the hydrate equilibrium curve towards lower temperatures. Winterization efficacy for a given PoHF can be expressed in terms of temperature difference, which can be directly related to the temperature shift of the hydrate equilibrium curve due to inhibition.

Using Eq. 3-9, the efficacy of winterization is expressed in terms of temperature difference as follows:

$$PoHF = \Phi \left( \frac{(\Delta T_{min} - W_e) - \mu}{\sigma} \right)$$

Where,  $\Delta T_{min} = |T_{L-min} - T_{eq}| = 44 \text{ } ^\circ\text{C}$ ,  $\mu = |-28.5 - 12.5| = 41 \text{ } ^\circ\text{C}$  and  $\sigma = (1.5^2 + 1.2^2)^{1/2} = 1.92 \text{ } ^\circ\text{C}$ ,

Therefore,

$$0.01 = \Phi \left( \frac{44 - W_e - 41}{1.92} \right)$$

$$W_e = \Delta T = 7.464 \text{ } ^\circ\text{C}$$

Then the required methanol concentration in weight percent in the aqueous phase is calculated using Eq.3-5:

$$7.464 = \frac{K_H W}{M(100 - W)}$$

$$W = 15.6 \text{ wt\% MeOH}$$

Therefore, using a methanol concentration of 15.6 in weight percent in the aqueous phase, the likelihood of hydrate formation is reduced from 0.94 to an acceptable value of 0.01.

### 3.4.3 Determination of heat trace capacity and insulation thickness

Suppose a natural gas pipeline exposed to a low temperature environment requires winterization with heat tracing and insulation. If a PoHF value of 0.001 is selected based

on acceptable risk values, a tradeoff between the heat tracing requirement and insulation thickness can be carried out through the following steps using the parameters given in

Table 3-1:

Table 3-1: Parameters used in case study

Pipe (3in)	Material	Stainless steel
	Inner diameter (in)	3.07
	Outer diameter (in)	3.5
	Thermal conductivity (W/m.K)	43
Insulation	Material	Calcium silicate
	Thermal conductivity (W/m.K)	0.04
Operating conditions	Temperature (°C)	N~( $\mu=12.5$ , $\sigma=1.5$ )
	Pressure (psi)	N~( $\mu=1025$ , $\sigma=60$ )
Ambient conditions	Temperature (°C)	N~( $\mu=-28.5$ , $\sigma=1.2$ )
Wind speed	Cross flow ( $\text{ms}^{-1}$ )	20
Gas	Composition	CH <sub>4</sub> : 99%, C <sub>2</sub> H <sub>6</sub> : 1%
	Velocity ( $\text{ms}^{-1}$ )	4.6

- a.) Develop the hydrate equilibrium curve for the given composition and calculate  $|\Delta T_{\min}|$  for a desired confidence interval (99%) following the steps given in Figure 3-3.

$$\Delta T_{\min} = 44 \text{ } ^\circ\text{C}$$

b.) Calculate the efficacy of winterization using Eq. 3-9:

$$PoHF = \Phi \left( \frac{(\Delta T_{min} - W_e) - \mu}{\sigma} \right)$$

Where,  $\Delta T_{min} = |T_{L-min} - T_{eq}| = 44 \text{ } ^\circ\text{C}$ ,  $\mu = |-28.5 - 12.5| = 41 \text{ } ^\circ\text{C}$  and  $\sigma = (1.5^2 + 1.2^2)^{1/2} = 1.92 \text{ } ^\circ\text{C}$ ,

Then,

$$0.001 = \Phi \left( \frac{44 - W_e - 41}{1.92} \right)$$

$$W_e = \Delta T = 8.933 \text{ } ^\circ\text{C}$$

Therefore, a winterization scheme with a thermal efficacy of 8.933 °C is required.

c.) Calculate heat transfer coefficients:

To calculate the heat transfer coefficient of air due to forced convection, first the Nusselt number should be calculated using Eq. 3-12 where all the properties are evaluated at film temperature (mean boundary layer temperature). A spreadsheet is developed where values for cladding/insulation surface temperature and steel pipe surface temperature are initially assumed to find the film temperature through an iterative process. Accounting for both external and internal heat transfer coefficients (Eq. 3-12, Eq. 3-16) and for a fixed insulation thickness, heat flow through insulation is estimated. Then a revised estimate for surface and interface temperature is made. The aforementioned process is repeated till there is negligible difference in temperature with a converged overall heat transfer coefficient.

d.) Calculate required wattage:

Then the required wattage (W/m) of the heat trace is calculated using the following:

$$Q = U * W_e * 2\pi * D_3$$

Following the same procedure, the heat trace requirement is calculated for different insulation thicknesses and plotted in Figure 3-8. Using Figure 3-8, a tradeoff between insulation thickness and heat trace capacity can be made considering various factors that affect the selection criteria. Though application costs may have a major influence on the tradeoff between these two winterization schemes, other factors such as corrosion issues and maintenance costs may also affect the selection criteria, since thicker insulation may lead to higher maintenance costs and downtime.

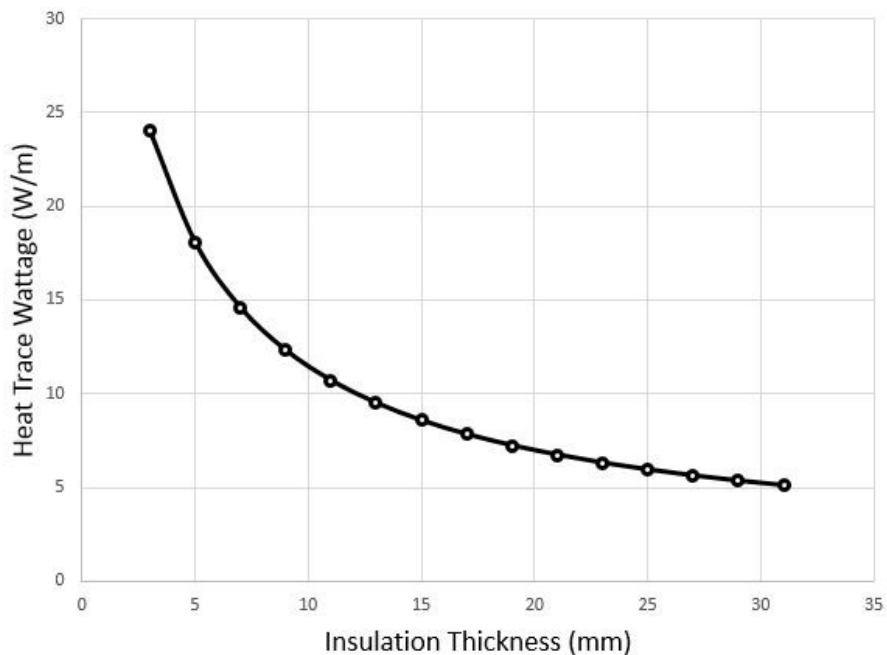


Figure 3-8: Insulation Thickness Vs Heat Trace Wattage

As shown in Figure 3-8, the heat trace wattage requirement drops exponentially with increasing insulation thickness. For insulation thickness greater than 20mm, the heat trace wattage requirement drops at an insignificant rate; 0.25 W/m per 1mm of insulation thickness. Also, for insulation thickness less than 10mm, the heat trace wattage requirement increases drastically. Therefore, it is recommended to select an insulation thickness in the range of 10-20mm with the corresponding heat trace wattage as illustrated in Figure 3-8. This decreases the initial PoHF value of 0.94 to the desired value of 0.001 which satisfies the acceptable risk levels.

If heat trace is selected as the sole winterization method, a very high heat trace capacity (~50 W/m) is required to satisfy the acceptable risk levels, due to the excessive heat loss from a bare pipe without insulation. Since the cost per meter of heat trace cable increases with heat trace capacity (W/m), adapting heat trace as the sole winterization scheme is not economically feasible. Therefore, a combined winterization strategy; heat trace with insulation is recommended to prevent hydrate formation.

### **3.5 Discussion**

A novel risk-based winterization approach is proposed to prevent hydrate formation in natural gas pipelines operating in northern harsh environments. The major steps of the proposed method are highlighted in Figure 3-3 and are described in detail in Section 3.3. As the initial step, the criticality of the selected pipeline is determined using severity values assigned to each consequence based on factors such as injuries/fatalities, environmental

damage, financial losses and loss of productivity. Then environment load is estimated for the region considered and expressed in probabilistic distributions. A novel method to estimate the probability of hydrate formation is presented in detail in Section 3.3.3, adapting limit state theory to calculate the PoHF. The next step involves estimating risk using the PoHF value calculated, for a known severity value. A risk matrix (Figure 3-4) is adapted to define the acceptable risk level for the system considered. If the estimated risk is not within the acceptable range, winterization efficacy ( $W_e$ ) is calculated for the maximum acceptable PoHF value.  $W_e$  is expressed in terms of temperature difference and depicts the winterization requirement. Section 3.4 illustrates the procedures to follow in determining parameters of winterization: insulation thickness, heat trace capacity and inhibitor percentage through examples. The inhibition requirement is determined using the Hammerschmidt equation (Eq. 3-5), where  $W_e$  is directly related to the temperature shift of the hydrate equilibrium curve due to inhibition. To determine insulation thickness and heat trace capacity,  $W_e$  is related to heat transfer equations. The example in Section 3.4.3 illustrates steps in detail to determine the insulation thickness and heat trace capacity for a desired PoHF based on acceptable risk values. Following the example, the initial value for probability of hydrate formation (0.94) is reduced to the desired value of 0.001, adapting a combined winterization strategy with parameters shown in Figure 3-8. Therefore, the initial high risk is reduced to an acceptable low value.

### 3.6 Conclusions

Formation of hydrates is a major flow assurance problem in natural gas pipelines. Winterization schemes can be adapted for pipelines in Arctic environments to avert the undesirable phenomenon of hydrate formation. Many factors influence the selection process of winterization schemes such as: safety, reliability, cost, environment, desired accuracy of temperature control and ease of implementation and control. The harsh environmental conditions in Arctic regions demand for more robust strategy in selecting winterization schemes than conventional methods do. A new method is developed to calculate the probability of hydrate formation and its associated risk for a given loading scenario where the winterization requirement is determined based on estimated risk. The proposed method is extended to a tradeoff between available winterization schemes in selecting the optimal scheme, based on acceptable risk levels. Validation of the methodology is carried out through its application in identifying inhibitor percentage, insulation thickness and heat trace wattage requirements for a natural gas pipeline. The addition of inhibitors changes properties of the flowing fluid to shift the hydrate forming curve to lower temperatures, whereas heat trace and insulation reduce heat loss to maintain operating conditions within the hydrate-free region. If inhibition is used as the sole winterization strategy, operating conditions may fall into the hydrate forming region at a certain point along the pipe's length due to heat loss. Therefore, inhibition with insulation and heat trace would provide a better solution for hydrate prevention than adapting individual winterization schemes, in terms of safety, risk and cost.

In the present work, wind velocity is considered a constant for ease of model development. Hence in future work, wind distribution modelling can be carried out to improve the proposed model and minimize limitations. As mentioned in the methodology, the present work is focused on reducing the likelihood of hydrate formation, rather than consequence assessment. Therefore, to expand the current model, a more robust quantitative approach can be used for consequence assessment instead of a qualitative approach. Moreover, the proposed method which carries out technical design calculations in selecting parameters of winterization schemes can be further expanded by evaluating the economic feasibility and applicability of winterization schemes. Therefore, future work will be carried out to improve the proposed method by adapting the aforementioned factors in selecting winterization schemes and their respective parameters.

### 3.7 References

- Baen, P., & Oldford, D. (2014). Surface heating for Arctic vessels and structures to prevent snow and ice accumulation. In *Petroleum and Chemical Industry Conference Europe, 2014* (pp. 1–10).  
<http://doi.org/10.1109/PCICEurope.2014.6900066>
- Brazil, H., Conachey, B., Savage, G., & Baen, P. (2012). Electrical heat tracing for surface heating on arctic vessels amp; structures to prevent snow and ice accumulation. In *2012 Record of Conference Papers Industry Applications Society 59th Annual IEEE Petroleum and Chemical Industry Technical Conference (PCIC)* (pp. 1–8). <http://doi.org/10.1109/PCICON.2012.6549665>
- Brazil, H., Conachey, R., Savage, G., & Baen, P. (2013). Electrical Heat Tracing for Surface Heating on Arctic Vessels and Structures to Prevent Snow and Ice Accumulation. *IEEE Transactions on Industry Applications*, 49(6), 2466–2470.  
<http://doi.org/10.1109/TIA.2013.2263372>
- Carson, D. B., & Katz, D. L. (1942). Natural Gas Hydrates. *Transactions of the AIME*, 146, 150.
- Churchill, S. W., & Bernstein, M. (1977). A Correlating Equation for Forced Convection From Gases and Liquids to a Circular Cylinder in Crossflow. *Journal of Heat Transfer*, 99(2), 300–306. <http://doi.org/10.1115/1.3450685>
- Elgibaly, A. A., & Elkamel, A. M. (1998). A new correlation for predicting hydrate formation conditions for various gas mixtures and inhibitors. *Fluid Phase Equilibria*, 152(1), 23–42. [http://doi.org/10.1016/S0378-3812\(98\)00368-9](http://doi.org/10.1016/S0378-3812(98)00368-9)

- Hammerschmidt, E. G. (1934). Formation of Gas Hydrates in Natural Gas Transmission Lines. *Industrial & Engineering Chemistry*, 26(8), 851–855.  
<http://doi.org/10.1021/ie50296a010>
- Lienhard IV, J. H., & Lienhard V, J. H. (2003). *A Heat Transfer Textbook, Third Edition*. Cambridge, Mass.: Phlogiston Press.
- Mokhatab, S., & Towler, B. (2005). Quickly estimate hydrate formation conditions in natural gases. *Hydrocarbon Processing*, 61–2.
- Motiee, M. (1991). Estimate Possibility of Hydrates. *Hydrocarbon Processing*, 70(7), 98–99.
- Nielsen, R. B., & Bucklin, R. W. (1983). Why Not Use Methanol for Hydrate Control? *Hydrocarbon Processing*, 62(4), 71.
- Notz, P. K. (1994). Discussion of the Paper “The Study of Separation of Nitrogen from Methane by Hydrate Formation Using a Novel Apparatus.” *Annals of the New York Academy of Sciences*, 715(1), 425–429. <http://doi.org/10.1111/j.1749-6632.1994.tb38855.x>
- Sloan, E. D. (1998). *Clathrate Hydrates of Natural Gases, Second Edition, Revised and Expanded*. CRC Press.
- Sloan, E. D. (2003). Fundamental principles and applications of natural gas hydrates. *Nature*, 426(6964), 353–363. <http://doi.org/10.1038/nature02135>
- Sloan, Jr, E. D., & Koh, C. (2007). *Clathrate Hydrates of Natural Gases, Third Edition*. CRC Press.

Sulistiyono, H., Lye, L. M., Khan, F. I., Yang, M., Oldford, D., & Dolny, J. (2014).

Estimating design temperatures in Arctic environments: A new approach. In *Oceans - St. John's, 2014* (pp. 1–5).

<http://doi.org/10.1109/OCEANS.2014.7002975>

The challenges facing arctic pipelines. (n.d.). Retrieved December 28, 2014, from

<http://www.offshore-mag.com/articles/print/volume-67/issue-9/construction-installation/the-challenges-facing-arctic-pipelines.html>

Yang, M., & Khan, F. I. (2013). Risk-based winterization for vessels operations in Arctic environments. *Journal of Ship Production and Design*, 29(4), 199–210.

<http://doi.org/10.5957/JSPD.29.4.120059>

# **Chapter 4. Multiphase Hydrate Induction Experiment in a Subsea Pipeline**

Dinesh Herath, Samith Rathnayaka, M.A. Rahman, Faisal Khan

*Safety and Risk Engineering Group (SREG), Faculty of Engineering and Applied Science, Memorial University of Newfoundland, St. John's, NL, Canada*

## **Abstract**

Formation of hydrates is one of the many challenges faced in the offshore oil and gas industry. It may result in blockage of subsea pipelines and equipment, which may result in flow line rupture and process accident. Although extensive experiment study is conducted to better understand the nucleation of hydrates and their slug flow behavior in gas-water/oil systems, there is limited understanding regarding the effects of multiphase fluid dynamics and geometric scales on the formation/growth of hydrates in subsea pipelines. In this paper, a multiphase lab scale flow loop set-up is proposed to study the effects of pipe diameter, wall roughness, solid particles and hydrodynamic properties. The multiphase development length of a pipe for varying geometric and flow parameters is also analyzed considering three phase mixture properties. This study will help in identifying the accurate development length for gas/liquid/solid multiphase flow.

Keywords: Hydrate flow loop, Development length, Three-phase Reynolds number, Induction time

## Nomenclature

$A$	Area (m <sup>2</sup> )
$C$	Solid concentration (%)
$D$	Pipe diameter (m)
$S$	Slip ratio
$x$	Mass quality
$\dot{M}_{(y)}$	Local mass flow rate (kgs <sup>-1</sup> )
$Re_m$	Homogeneous Reynolds number
$u_{(y)}$	Local velocity (ms <sup>-1</sup> )
$\rho_{(y)}$	Local density (kgm <sup>-3</sup> )
$\mu_{(y)}$	Local viscosity (Pas)
$u_{3-p}$	Three-phase mixture velocity (ms <sup>-1</sup> )
$\rho_{3-p}$	Three-phase homogeneous density (kgm <sup>-3</sup> )
$\mu_{3-p}$	Three-phase homogeneous viscosity (Pas)
$\alpha$	Void fraction
$\varphi$	Volumetric concentration
$u_{(y)}^S$	Local superficial velocity (ms <sup>-1</sup> )

### 4.1 Introduction

Formation of hydrates is considered as one of the many challenges faced in the oil and gas industry, where hydrate formation may lead to blockage of pipelines and equipment. For

natural gas pipelines, these blockages may lead to large plugs, which make the pipelines more susceptible for burst and explosion, exposing a huge safety concern.

Extensive research has been carried regarding hydrate formation during the last two decades and several conceptual models have been developed to better understand the nucleation of hydrates (Zerpa, Sloan, Sum, & Koh, 2012). Several flow loops dedicated to hydrate research can be also found in literature. Mauricio et al. (Di Lorenzo Ruggeri, Seo, & Sanchez Soto, 2012) summarized information of the available hydrate flow loops. *Hytra* flow loop consists of a 40m long test section and has the capability of supporting gas volume fractions higher than 90% (Di Lorenzo & Sanchez, n.d.). Xiaofang et al. (Lv et al., 2012) conducted experiments using a high-pressure hydrate experimental loop developed by multiphase-flow research group at China University of Petroleum, to better understand hydrate-slurry flow. Similar to other experiments carried out related to hydrate formation, they did not study the effect of solid particles on hydrate formation. Induction time of gas hydrate crystallization is an important area of research due to its association with kinematic inhibitors. Therefore, different models have been developed to calculate hydrate induction time (Kashchiev & Firoozabadi, 2003), (Kashchiev, 2000). Figure 4-1 illustrates the basic process flow chart for a conventional hydrate flow loop which supports liquid-liquid-gas (L-L-G) flow. It is important to note the use of three phase separators in these flow loops where gas, oil and water mixture is separated at the test section outlet and circulated back to the loop. This will increase the time required for the system to reach hydrate forming temperature.

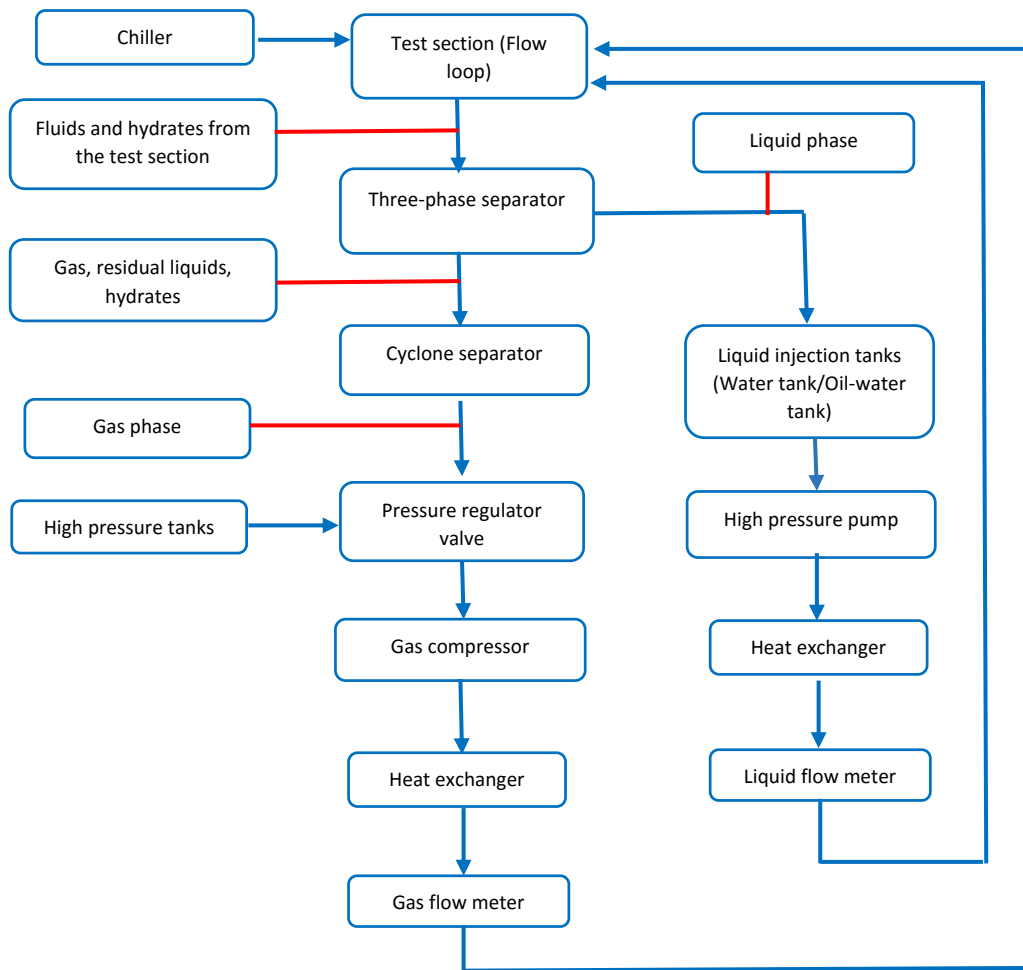


Figure 4-1: Basic process flow chart of multiphase flow loop and hydrate induction experiment

Although many experimental studies related to hydrate formation in two-phase flow and three-phase flow (L-L-G) have been carried out, there are no experimental studies performed to study the effects of solid particles on formation of hydrates as per authors' knowledge. Therefore the present study aims to study the effects of solid particles on hydrate formation using the proposed three-phase hydrate flow loop. It is of topmost importance to define process parameters prior to the design stage of flow loop. Therefore to determine the pressure and temperature conditions of hydrate formation for any given

composition, general process simulation tools which have the capability of predicting hydrate forming conditions such as *PVTsim*, *Hysys*, *PIPESIM* can be used. Moreover, there are tools which have been specifically developed for hydrate calculations such as *CSMHYD* (Sloan, 1998).

One of the main objectives of this work is to develop a lab-scale flow loop which supports three-phase flow, solid-liquid-gas (S-L-G). Since length of the test section will be restrained, in order to obtain accurate pressure values the positioning of pressure transmitters and other probes should be placed at locations where the fully developed flow regime exists. On the other hand, if a measurement device is placed within the development length of the pipe, it will display erroneous measurement values. Hence, development length is a significant parameter which plays a vital role during flow loop design stage. Moreover, the development length of a single phase flow is well understood. In case of multiphase flow there is no correlation or model exists to accurately predict the development length. Thus, in this study a novel approach is taken to better understand the multiphase development length in a pipe.

## **4.2 Lab-Scale Flow Loop**

The proposed hydrate-flow loop is designed as a lab-scale loop which supports three-phase flow as shown in Figure 4-2. Unlike in conventional hydrate flow loops (Figure 4-1), the proposed multiphase hydrate flow loop does not require a three-phase separator due to the continuous flow design. Therefore, time required to reach steady state flow conditions will be reduced drastically. Water and gas are injected separately to the test section and the flow

is implemented by means of an in-line screw pump. Solid particles are introduced to the flow through a separate port (S). Formation of hydrates can be observed through the view ports (V1, V2) installed at two different locations.

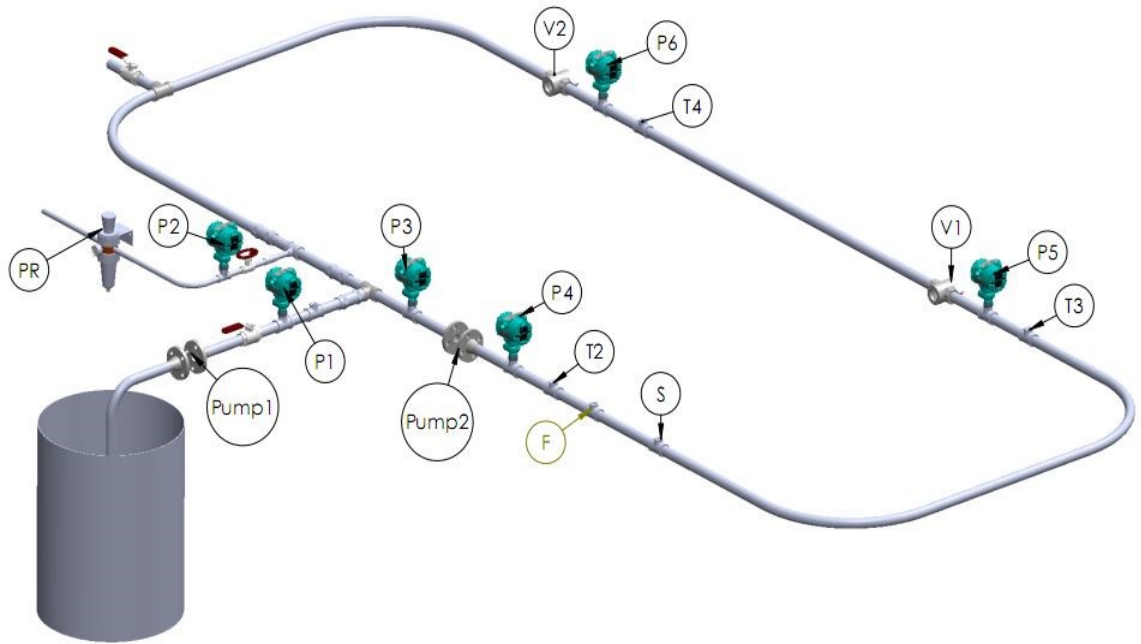


Figure 4-2: Process flow diagram of proposed flow loop PR-Pressure Regulator; F-Flow Meter, P-Pressure Transmitter; T-Temperature Transmitter; S-Solid Particles; V-View Port

When hydrate crystallization/nucleation occurs, a sudden pressure drop and a temperature rise can be observed. This can be used to determine the exact time for hydrate formation, once the flow loop has reached hydrate forming temperature and pressure conditions. The pressure drop is due to the consumption of gas former during hydrate formation, while the temperature rise is due to the exothermic behavior of hydrate forming reaction (Mork, 2003).

The pressure drop along the length of the test section is an important parameter to be determined which assists in the pump selection process. It also provides information about the pressure abnormality in the flow line due to hydrate particle blockage. Since the proposed hydrate-flow loop only consists of horizontal test pipe sections, frictional pressure drop will be the main contributor for pressure drop. Development length (entrance length) of the flow is another important parameter which may affect the induction time of hydrates. Previous studies reported in this area of research cannot predict all the hydrodynamic effects related to hydrate formation. Both frictional pressure drop and development length are expressed as functions of the non-dimensional parameter, Reynolds number. Therefore, current work will be focused on studying the effects of flow parameters on three-phase development length.

### 4.3 Development Length

Development length, also referred to as entrance length can be defined as the length until the flow velocity profile is fully developed. Durst et al. (Durst, Ray, Ünsal, & Bayoumi, 2005) proposed a correlation for development length for laminar flow as follows.

$$\frac{L}{D} = [(0.619)^{1.6} + (0.0567Re)^{1.6}]^{1/1.6} \quad (4-1)$$

For turbulent flow,

$$\frac{L}{D} = 4.4Re^{1/6} \quad (4-2)$$

As development length of flow is expressed as a function of Reynolds number (Eq. 4-1, Eq. 4-2), the following sections of the paper will focus on defining a three-phase Reynolds number by adopting a homogeneous model. Furthermore, the effect of fluid and flow parameters such as velocity, density, viscosity, solid concentration as well as geometric parameters (pipe diameter) on development length will be discussed.

#### 4.3.1 Homogeneous Reynolds number

The general expression of Reynolds number for homogeneous flow can be expressed as a function of homogeneous density ( $\rho_m$ ), mixture velocity ( $u_m$ ), pipe diameter ( $d$ ), and homogeneous viscosity ( $\mu_m$ ).

$$Re_m = \frac{\rho_m u_m D}{\mu_m} \quad (4-3)$$

Homogeneous density can be expressed as a function of void fraction ( $\alpha$ ) as follows:

$$\rho_m = \rho_l(1 - \alpha) + \rho_g \alpha \quad (4-4)$$

Void fraction can be expressed as follows:

$$\alpha = \frac{1}{1 + \left[ \left( \frac{u_g}{u_l} \right) \left( \frac{1-x}{x} \right) \left( \frac{\rho_g}{\rho_l} \right) \right]} \quad (4-5)$$

For a homogeneous model, the above expression can be simplified by substituting the slip ratio ( $u_g/u_l$ ) equal to 1 (no slip condition). In fluid dynamics, there are several commonly used expressions to determine two-phase viscosity of gas-liquid flow, where most of these expressions are functions of mass quality ( $x$ ).

$$\mu_m = \left( \frac{x}{\mu_g} + \frac{1-x}{\mu_l} \right)^{-1} \quad (\text{McAdams et al. (McAdams, Woods, \& Heroman, 1942)}) \quad (4-6)$$

$$\mu_m = \mu_l(1-x) + \mu_g x \quad (\text{Cicchitti et al. (Cicchitti, Lombardi, Silvestri, Soldaini, \& Zavattarelli, 1959)}) \quad (4-7)$$

$$\mu_m = \rho_m \left[ x \frac{\mu_g}{\rho_g} + (1-x) \left( \frac{\mu_l}{\rho_l} \right) \right] \quad (\text{Dukler et al. (Dukler, Wicks, \& Cleveland, 1964)}) \quad (4-8)$$

$$\mu_m = \mu_l(1-\alpha)(1+2.5\alpha) + \mu_g \alpha \quad (\text{Beattie and Whalley (Beattie \& Whalley, 1982)}) \quad (4-9)$$

Mixture velocity ( $u_m$ ) can be expressed in terms of superficial velocities of the respective phases.

$$u_m = u_g^s + u_l^s \quad (4-10)$$

### 4.3.2 Three-phase Reynolds number

Since there is no available expression/relationship for three-phase Reynolds number, the expression for homogeneous Reynolds number will be utilized in developing a three-phase Reynolds number which considers slurry flow (liquid and solid) and gas flow as two phases. Three-phase flow can be considered as a combination of liquid, solid and gas flow. Therefore, if liquid and solid phases are considered as one homogeneous slurry phase, three-phase flow can be effectively expressed in terms of two-phase flow expressions by replacing the liquid phase characteristics by slurry flow characteristics.

Homogeneous three-phase density can be obtained from,

$$\rho_{3-p} = \rho_{sl}(1 - \alpha) + \rho_g \alpha \quad (4-11)$$

Where the void fraction is expressed as follows;

$$\alpha = \frac{1}{1 + \left[ \left( \frac{1-x}{x} \right) \left( \frac{\rho_g}{\rho_{sl}} \right) \right]} \quad (4-12)$$

Similarly, any one of the aforementioned expressions for two-phase viscosity can be used to define the three-phase viscosity as a function of slurry viscosity ( $\mu_{sl}$ ), gas viscosity ( $\mu_g$ ), and mass quality ( $x$ ). For the case of McAdams, three-phase viscosity can be expressed as follows,

$$\mu_{3-p} = \left( \frac{x}{\mu_g} + \frac{1-x}{\mu_{sl}} \right)^{-1} \quad (4-13)$$

Three-phase mixture velocity can be expressed in terms of superficial velocities of the respective phases.

$$u_{3-p} = u_g^s + u_{sl}^s \quad (4-14)$$

### 4.3.3 Slurry flow

A mixture of liquid and solid particles is known as slurry. There are different approaches available to describe the viscosity of a slurry flow. One of the earliest was proposed by Einstein (Einstein, 1989) for the viscosity of a system comprising of spheres suspended in liquid as a function of pure liquid viscosity ( $\mu_l$ ) and volumetric concentration ( $\varphi$ ). This laid the foundation for the development of many models for viscosity determination.

$$\frac{\mu_s}{\mu_l} = (1 + 2.5\varphi) \quad (4-15)$$

Eq. 4-15 does not consider the effect of particle size and interaction between other particles, which is considered to be a key limitation. Therefore, Thomas Equation (Thomas, 1965) which accounts for the interaction between solid particles is being widely used in the research area of ice-slurry (Kitanovski & Poredoš, 2002).

$$\frac{\mu_s}{\mu_l} = 1 + 2.5C + 10.05C^2 + 0.00273e^{16.6C} \quad (4-16)$$

This model considers the flow to be homogeneous and is valid for particle sizes in the range of 0.099 to 435  $\mu\text{m}$ .

#### 4.4 Results and Discussions

Development length was calculated at different slurry superficial velocities with varying flow parameters such as void fraction, solid concentration, pipe diameter, liquid and gas viscosities. Then the development length to diameter ratio was plotted against slurry superficial velocities to study the effects of varying flow parameters. The definition proposed by McAdams et al. (Eqn. (4-6)) is used to define 3-phase viscosity for all the calculations.

From Figure 4-3 it is observed that development length shows an increasing trend with liquid superficial velocity. Moreover, for increasing void fractions, development length increases due to enhanced inertial effects over the stratified effect. From Figure 4-3 it can be noted that, at  $U_{SL}^S = 2\text{ms}^{-1}$ , as void fraction ( $\alpha$ ) increases from 0.1-0.6,  $L/D$  increases by 0.99%. Whereas, when  $\alpha$  increases from 0.6-0.9,  $L/D$  increases by 4.6%, which shows an increasing trend.

The solid concentration shows a relationship with development length similar to that of void fraction. From Figure 4-3 it can be clearly seen that, as solid concentration increases, development length increases. As solid concentration increases, slurry viscosity increases, which in turn increases the three-phase viscosity. Similarly, homogeneous three-phase density increases with solid concentration. Though the percentage increase is high than that

of three-phase viscosity. Therefore, three-phase Reynolds number increases with solid concentration and results in higher development lengths. The level of increase of development length with solid concentration does not vary significantly. The graph (Figure 4-4) shows 3.7% increase for concentration change from 0.2-0.4 and 3.75% from 0.6-0.9.

For varying pipe diameters, from Figure 4-5 it can be seen that the entrance length increases with the pipe diameter in a similar manner compared to void fraction and solid concentration, since Reynolds number is directly proportional to pipe diameter.

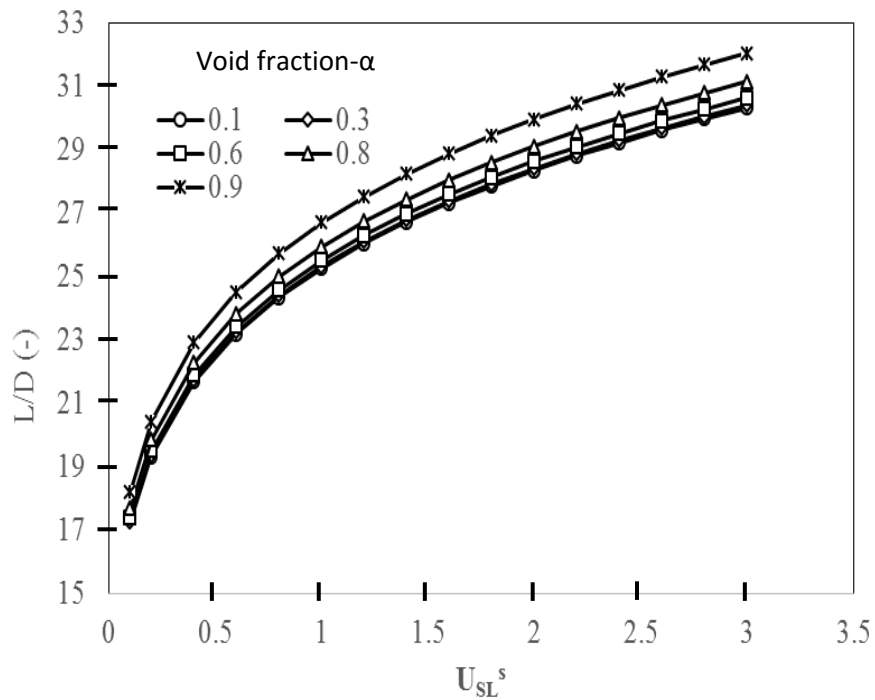


Figure 4-3: Slurry superficial velocity Vs ratio of entrance length to pipe diameter with varying void fractions

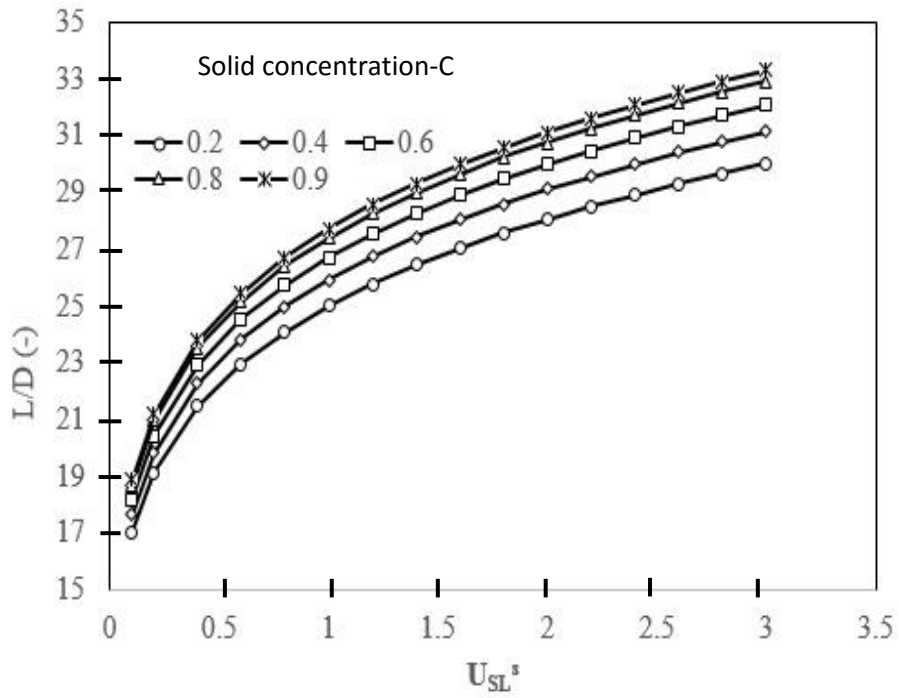


Figure 4-4: Slurry superficial velocity Vs ratio of entrance length to pipe diameter with varying solid concentrations

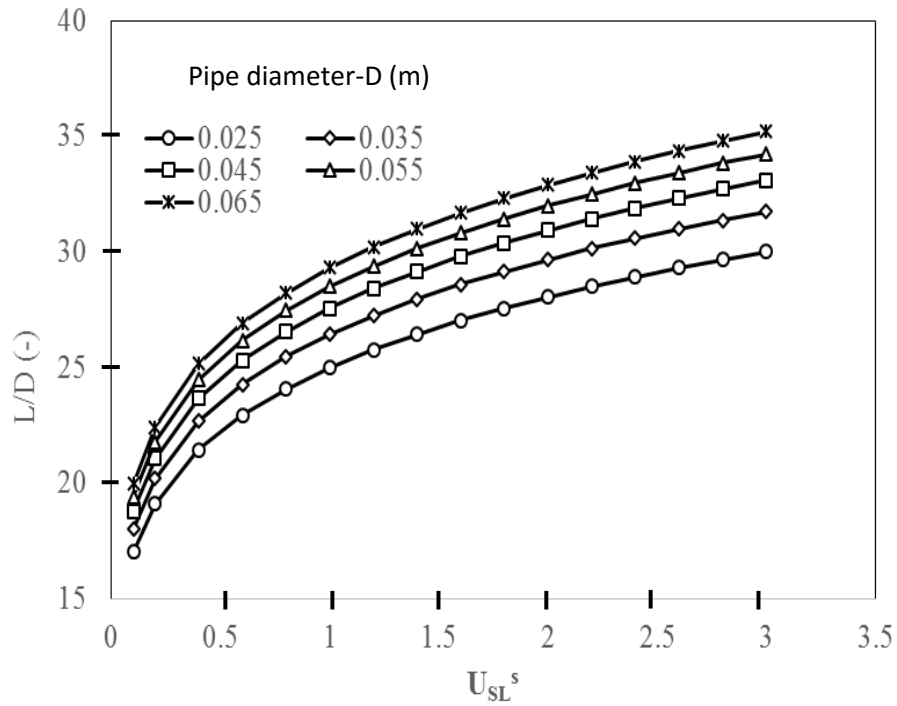


Figure 4-5: Slurry superficial velocity ratio Vs Entrance length to pipe diameter with varying pipe diameters

Development length shows a decreasing trend with liquid viscosity (Figure 4-6), as opposed to void fraction, solid concentration and pipe diameter, since viscosity is inversely proportional to Reynolds number. Viscosity tries to suppress the turbulent eddies, making the streamline of the flow as parallel as possible. From Figure 4-6, entrance length displays 18.4% decrement when viscosity changes from 0.001 Pas to 0.004 Pas, while 6.8% decrement when viscosity changes from 0.004 Pas to 0.008 Pas (at  $U_{SL}^S = 2ms^{-1}$ ).

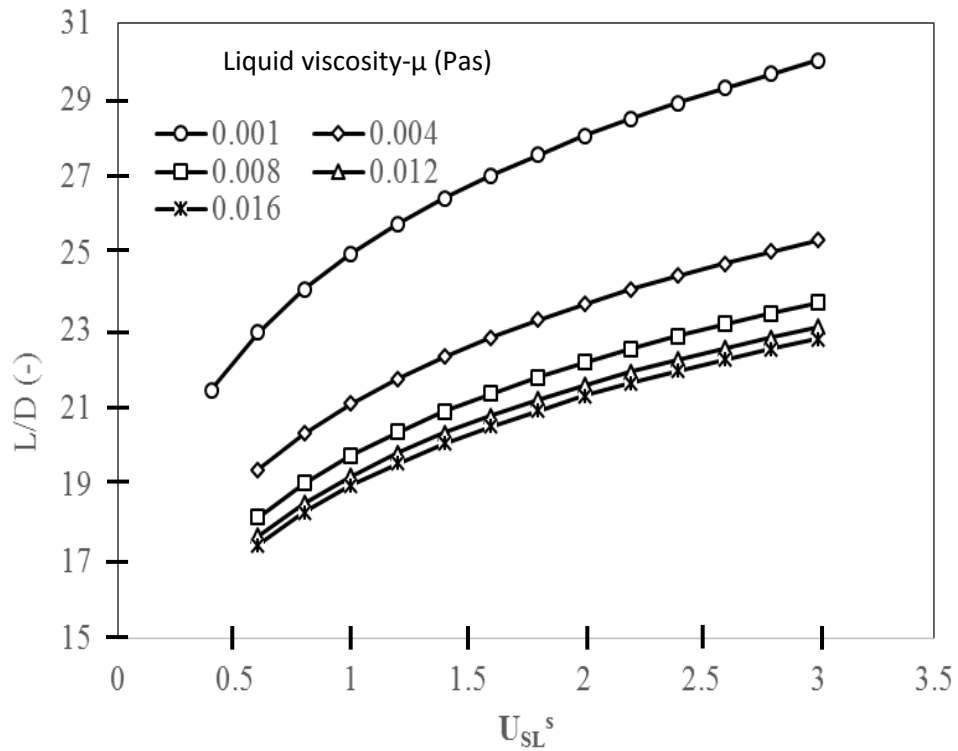


Figure 4-6: Slurry superficial velocity Vs ratio of entrance length to pipe diameter with varying liquid viscosity

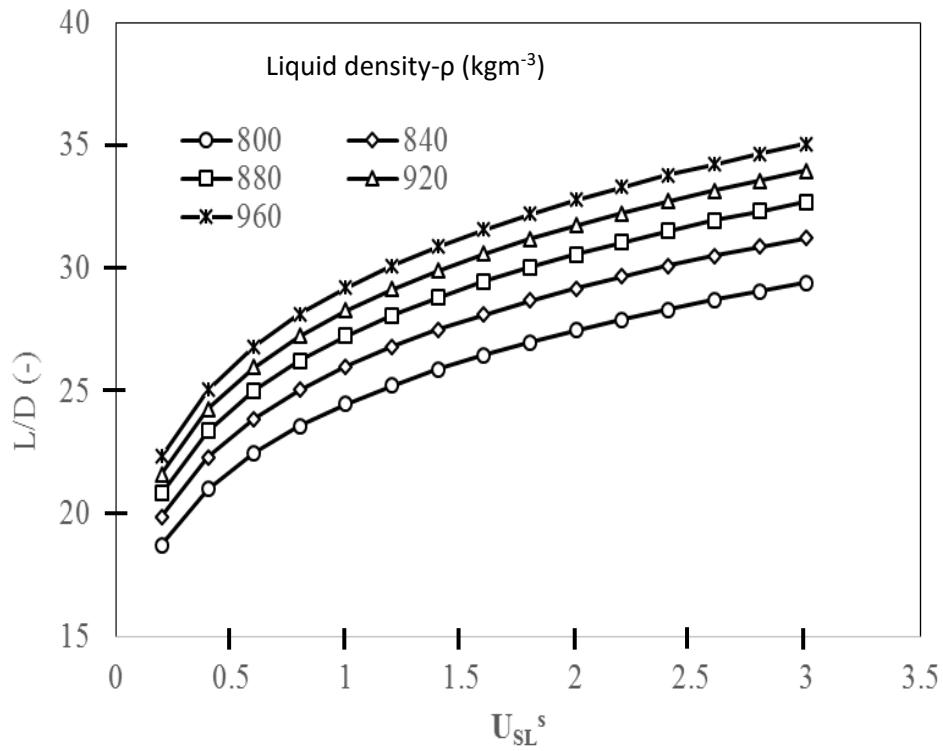


Figure 4-7: Slurry superficial velocity Vs ratio of entrance length to pipe diameter with varying liquid density

Similar to the case of the pipe diameter, the development length increases with increasing liquid density for any fixed slurry superficial velocity. As liquid density increases, slurry density increases, which in turn increases homogeneous density. Since Reynolds number is proportional to density, development length increases with liquid density. From Figure 4-7 it can also be noted that, percentage increase of development length does not vary significantly with increasing diameter.

## 4.5 Conclusions

A multiphase hydrate flow loop is proposed to study the effects of geometric and hydrodynamic parameters on hydrate formation. Due to the significance of the parameter-development length in flow loop design, a novel approach is taken to better understand the multiphase development length in a pipeline. The effects of different flow parameters such as void fraction, solid concentration, liquid viscosity, liquid density and geometric parameters such as pipe diameter on three-phase development length were studied, assuming homogeneous flow behavior. It is evident that the rate of increase of development length drops with increasing void fractions, while the opposite was observed for the case of solid concentration. If liquid viscosity is increased, the development length decreases exponentially as viscosity tries to suppress the turbulent eddies, making the streamline of flow as parallel as possible.

The analysis carried out in this work does not account for the hydrate formation mechanisms: the chemistry behind hydrate formation reactions, heat transfer and thermodynamics. Therefore, in future work all of the aforementioned factors which affect hydrate formation will be taken into consideration and validated through experiments carried out using the proposed multiphase hydrate flow loop. Also, the influence of solid particles on hydrate induction time will be studied as future work.

#### 4.6 References

- Beattie, D. R. H., & Whalley, P. B. (1982). A simple two-phase frictional pressure drop calculation method. *International Journal of Multiphase Flow*, 8(1), 83–87.  
[http://doi.org/10.1016/0301-9322\(82\)90009-X](http://doi.org/10.1016/0301-9322(82)90009-X)
- Cicchitti, A., Lombardi, C., Silvestri, M., Soldaini, G., & Zavattarelli, R. (1959). *Two-Phase Cooling Experiments: Pressure Drop, Heat Transfer and Burnout Measurements* (No. CISE-71). Centro Informazioni Studi Esperienze, Milan.  
Retrieved from <http://www.osti.gov/scitech/biblio/4181977>
- Di Lorenzo, M., & Sanchez, G. (n.d.). *Experimental study of the flow behaviour of a gas hydrate system in the Hytra Loop* (No. EP-12-07-12-37). Australia: CSIRO Earth Science and Resource Engineering.
- Di Lorenzo Ruggeri, M., Seo, Y., & Sanchez Soto, G. (2012). The CSIRO's hydrates flow loop as a tool to investigate hydrate behaviour in gas dominant flows. Presented at the Proceedings of the 7th International Conference on Gas Hydrates, Edinburgh, Scotland, United Kingdom: ICGH Conference. Retrieved from <http://www.pet.hw.ac.uk/icgh7/papers/icgh2011Final00516.pdf>
- Dukler, A. E., Wicks, M., & Cleveland, R. G. (1964). Frictional pressure drop in two-phase flow: A. A comparison of existing correlations for pressure loss and holdup. *AIChE Journal*, 10(1), 38–43. <http://doi.org/10.1002/aic.690100117>
- Durst, F., Ray, S., Ünsal, B., & Bayoumi, O. A. (2005). The Development Lengths of Laminar Pipe and Channel Flows. *Journal of Fluids Engineering*, 127(6), 1154–1160. <http://doi.org/10.1115/1.2063088>

- Einstein, A. (1989). *The Collected Papers of Albert Einstein*. Princeton University Press.
- Kashchiev, D. (Ed.). (2000). Author index. In *Nucleation* (pp. 515–523). Oxford: Butterworth-Heinemann. Retrieved from <http://www.sciencedirect.com/science/article/pii/B9780750646826500391>
- Kashchiev, D., & Firoozabadi, A. (2003). Induction time in crystallization of gas hydrates. *Journal of Crystal Growth*, 250(3–4), 499–515. [http://doi.org/10.1016/S0022-0248\(02\)02461-2](http://doi.org/10.1016/S0022-0248(02)02461-2)
- Kitanovski, A., & Poredoš, A. (2002). Concentration distribution and viscosity of ice-slurry in heterogeneous flow. *International Journal of Refrigeration*, 25(6), 827–835. [http://doi.org/10.1016/S0140-7007\(01\)00091-3](http://doi.org/10.1016/S0140-7007(01)00091-3)
- Lv, X., Gong, J., Li, W., Shi, B., Yu, D., & Wu, H. (2012). Experimental Study on Natural Gas Hydrate Slurry Flow. Society of Petroleum Engineers. <http://doi.org/10.2118/158597-MS>
- McAdams, W. H., Woods, W. K., & Heroman, L. C. (1942). Vaporization inside horizontal tubes II-benzene-oil mixtures. *Transactions of the ASME*, 64(3), 193–200.
- Mork, M. (2003). *Formation rate of natural gas hydrate: Reactor experiments and models* (Dr.ing.). Norges teknisk-naturvitenskapelige universitet, Norway. Retrieved from <http://search.proquest.com/docview/305215297?accountid=12378>
- Sloan, E. D. (1998). *Clathrate Hydrates of Natural Gases, Second Edition, Revised and Expanded*. CRC Press.

- Thomas, D. G. (1965). Transport characteristics of suspension: VIII. A note on the viscosity of Newtonian suspensions of uniform spherical particles. *Journal of Colloid Science*, 20(3), 267–277. [http://doi.org/10.1016/0095-8522\(65\)90016-4](http://doi.org/10.1016/0095-8522(65)90016-4)
- Zerpa, L. E., Sloan, E. D., Sum, A. K., & Koh, C. A. (2012). Overview of CSMHyK: A transient hydrate formation model. *Journal of Petroleum Science and Engineering*, 98–99, 122–129. <http://doi.org/10.1016/j.petrol.2012.08.017>

## Chapter 5. Summary

In this study, a novel methodology is presented to assess the probability of hydrate formation in natural gas pipelines with a risk-based approach to determine the parameters of winterization schemes to prevent hydrate formation in natural gas pipelines operating in Arctic conditions. A lab-scale flow setup is also proposed to further extend the study to understand the effects of geometric and hydrodynamic parameters on hydrate formation.

Chapter 1 provided an extensive review on the natural phenomena of hydrate formation, including the characteristics of hydrates and calculation methods of hydrate equilibrium conditions with examples. It also described the typical hydrate forming conditions and hydrate forming points in subsea equipment of oil and gas industry. Hydrate prevention strategies which are currently being adapted by the oil and gas industry such as removal of water, inhibition and heat trace were also discussed here, providing calculation methods for determining the inhibitor percentage requirements.

Chapter 2 provided a novel methodology to assess the probability of hydrate formation in a subsea production and transportation system, for a given operating condition and composition. The work presented in this chapter focused only on the right-hand side of the hydrate forming curve (hydrate-free zone) and developed a methodology to quantify the likelihood of reaching hydrate-stable zone in probabilistic terms. The proposed method used Shortest Path of Hydrate Formation (SPHF), which considers all achievable pathways for any given operating point (temperature and pressure) to reach hydrate forming conditions. Validation of the method was carried out through obtaining a relationship

between the curves of similar probabilities for the two scenarios: with and without inhibition. From the results obtained, it was evident that the probability curves generated from the proposed method were correlated to the respective hydrate forming curves with a percentage deviation of less than 8% (considering the average temperature difference).

Chapter 3 provided a novel methodology to calculate the parameters of winterization for natural gas pipelines operating in Arctic conditions to avoid hydrate formation. In this study, a risk-based approach was proposed to calculate the parameters of winterization adapting a method based on limit-state theory to estimate the probability of hydrate formation. Different winterization strategies were discussed extensively and detailed steps were presented to determine the winterization parameters of inhibition, insulation and heat-trace. A combined-winterization approach was also proposed, which entailed trade-off between cost and effectiveness of the optimum winterization strategy.

Chapter 4 presented a lab-scale multiphase flow loop set-up to study the effect of geometric and hydrodynamic properties on hydrate formation. Due to the significance of the parameter- development length in flow loop design, a novel approach was presented to better understand the multiphase development length in a pipeline. A detailed analysis was carried out in the multiphase development length of a pipe for varying geometric and flow parameters: void fraction, solid concentration, pipe diameter, liquid viscosity and liquid density, assuming homogeneous flow. From the results obtained it was evident that the rate of increase of development length dropped with increasing void fractions, while the opposite was observed for the solid concentration. Also, the development length decreased

exponentially with increasing viscosity as viscosity tries to suppress the turbulent eddies, making the streamline of flow parallel as possible.

Recommendations for future work:

- Integrate updating mechanisms (ex: Bayesian probability theory) to achieve better approximations for the probability of hydrate formation.
- Account for wind distribution modelling to improve the risk-based winterization approach and minimize limitations.
- Adopt a more robust quantitative approach for consequence assessment instead of a qualitative approach.
- Consider economic feasibility and applicability of the winterization schemes when selecting the optimum combined-winterization approach.
- Study the effect of solid particles on hydrate formation through experiments.

## Appendix

### Appendix A: Parameters of combined winterization approach

<b>Insulation Thickness (mm)</b>	<b>Heat Trace Wattage (W/m)</b>
3	24.05
5	18.09
7	14.6
9	12.32
11	10.71
13	9.5
15	8.57
17	7.83
19	7.23
21	6.73
23	6.3
25	5.94
27	5.62
29	5.34
31	5.100

## Appendix B: Derivation of Equations

Mass quality is the ratio between gas mass flow rate and total mass flow rate.

$$x = \frac{\dot{M}_g}{\dot{M}_g + \dot{M}_l} \quad (\text{B-1})$$

Derivation of void fraction ( $\alpha$ ):

$$u_g = \frac{\dot{Q}_g}{A * \alpha} = \frac{(\dot{M}_g / \rho_g)}{A * \alpha} = \frac{\dot{M} * x}{A * \alpha * \rho_g} \quad (\text{B-2})$$

$$u_l = \frac{\dot{Q}_l}{A * (1 - \alpha)} = \frac{(\dot{M}_l / \rho_l)}{A * (1 - \alpha)} = \frac{\dot{M} * (1 - x)}{A * (1 - \alpha) * \rho_l} \quad (\text{B-3})$$

Equating the expressions for gas and liquid phase true velocities,

$$\alpha = \frac{1}{1 + \left[ \left( \frac{1-x}{x} \right) \left( \frac{\rho_g}{\rho_l} \right) \right]} \quad (\text{B-4})$$

Introducing the slip ratio factor where,

$$S = \frac{u_g}{u_l} \quad (\text{B-5})$$

The following relationship can be obtained,

$$\alpha = \frac{1}{1 + \left[ S \left( \frac{1-x}{x} \right) \left( \frac{\rho_g}{\rho_l} \right) \right]} \quad (\text{B-6})$$

### Superficial velocities

$$u_g^s = \frac{\dot{Q}_g}{A_{tot}} = \frac{x * \dot{M}}{A_{tot} * \rho_g} = \alpha * u_g \quad (\text{B-7})$$

$$u_l^s = \frac{\dot{Q}_l}{A_{tot}} = \frac{(1-x) * \dot{M}}{A_{tot} * \rho_l} = (1-\alpha) * u_l \quad (\text{B-8})$$

Modifying the above equations, we first define vapor quality in terms of gas and slurry (solid+liquid). Then define superficial velocity for slurry flow.

$$x = \frac{\dot{M}_g}{\dot{M}_g + \dot{M}_{sl}} \quad (\text{B-9})$$

$$u_{sl}^s = \frac{\dot{Q}_{sl}}{A_{tot}} = \frac{(1-x) * \dot{M}}{A_{tot} * \rho_{sl}} = (1-\alpha) * u_{sl} \quad (\text{B-10})$$

Therefore mean velocity of the three-phase flow can be defined from the summation of superficial velocities.

$$u_m = u_g^s + u_{sl}^s \quad (\text{B-11})$$